treated with individualized chemotherapy at Chiba University Hospital or Chiba Cancer Center Hospital from 1995 to 2004. All of the patients treated during this period were evaluated and included in the study without exclusion. The study protocol was approved by the institutional review board, and a written informed consent was obtained from all of the patients or a guardian. The patient characteristics are summarized in Table I. Magnetic resonance imaging (MRI), with and without gadolinium enhancement, was performed preoperatively and postoperatively before the initiation of radio-chemotherapy. Regarding extent of resection, the total/subtotal resection was defined as 90% or more reduction of the tumor volume in the postoperative MRI. The biopsy meant the CT-guided stereotactic needle biopsy, and partial removal covered all other situations. Toxicity was graded according to the National Cancer Institute's Common Toxicity Criteria version 3.0.

Drug sensitivity test (DST). Direct quantification of apoptosis by means of flow cytometric DNA analysis is widely used in basic research and has been successfully utilized for clinical DST (15-17). Cell suspensions prepared from surgically resected tumor tissues were incubated with each of 25 different anticancer drugs already being used in clinical practice (cyclophosphamide, ifosphamide, nimustine, ranimustine, cisplatin, carboplatin, adriamycin, daunomycin, pirarubicin, epirubicin, aclarubicin, mitoxantrone, etoposide, camptothecin, methotraxate, 5-fluorouracil, thioinosine, cytosine arabinoside, mitomycin C, bleomycin, vincristine, vinblastine, vindesine, paclitaxel and docetaxel). The *in vitro* drug concentrations were set both at the peak plasma concentration when the clinically recommended doses were provided and at 1/10 of that level (18). Drug-induced apoptosis was quantified with a flow cytometer (FACScan; Becton Dickinson, Mountain View, CA, USA) as the sub-G1 population. To confirm the presence of drug-induced apoptosis, morphological examinations of the nuclei were also performed on the same samples. DNA integrity assessed by the FCM analysis correlated well with the morphological changes in the nuclei.

Treatment protocols. For individualization of chemotherapy, the most effective drug *in vitro* was routinely selected as the key drug for each individual patient. In addition, one or two drugs were selected for combination with the key drug according to their degree of effectiveness and their mechanism of pharmaceutical action. The doses and schedules of chemotherapy regimens were determined on the basis of clinically recommended doses. When no agent was positive *in vitro*, the patients were treated with a modified PCV chemotherapy with substitution of lomustine with nimustine (nimustine 75 mg/m², vincristine 1 mg/m² and procarbazine 100 mg/day) (19). For all patients, the conventional 60-Gy radiotherapy with a megavoltage machine was started within 2 weeks of surgical removal in conjunction with the chemotherapy.

MGMT immunohistochemistry. For immunohistochemical analysis, paraffin-embedded samples were sliced and mounted on glass slides. Mouse monoclonal anti-MGMT antibody MT3.1 (1:200 dilution; Chemicon, Inc., Temecula, CA, USA) was used as the primary antibody. A heat-induced epitope was formed using microwaves in 10 mM citric acid buffer

Table I. Patient characteristics (n=74).

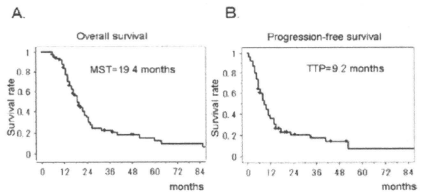| Age (years)	
Mean	51.5
Range	15-77
Gender	
Male	49 (66%)
Female	25 (34%)
Karnofsky performance score	
≥70	42 (57%)
<70	32 (43%)
Tumor location	
Left	37 (50%)
Right	28 (38%)
Midline	9 (12%)
Extent of surgery	
Total/Subtotal	46 (62%)
Partial/Biopsy	28 (38%)

Figure 1. Kaplan-Meier analyses of overall survival (A) and progression-free survival (B) in the patients with glioblastoma treated with individualized chemotherapy. MST, median survival time; TTP, time to tumor progression.

at pH 7.2. The samples were incubated with the antibody overnight in the same buffer followed by incubation with the biotinylated secondary antibody (1:500 dilution; Dako, Tokyo, Japan). The bound antibodies were visualized by the avidin biotinylated peroxidase complex method and diaminobenzidine tetrachloride (Santa Cruz Biotechnology, Inc., Santa Cruz, CA, USA). Human liver was used as the positive control, and the negative control was achieved by omitting the primary antibody from the procedure. Tissue specimens that showed staining of >10% of the malignant cells were considered positive for MGMT.

Statistical analysis. The primary end-point of this study was overall survival and the secondary end-points were progression-free survival and safety. Survival curves were generated using the Kaplan-Meier method, and the survival rates were compared with the log-rank test. The patient survival duration was calculated from the date of surgery until the date of last follow-up or death, and progression-free survival until the date of recurrence detection or until the last follow-up. The Fisher's exact probability test and χ^2 test were used to evaluate

Table II. Multivariate analyses for favorable prognostic factors.

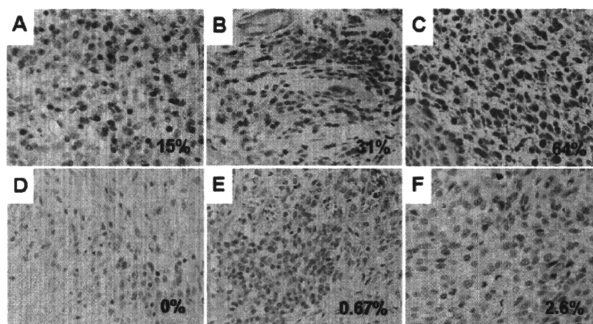|	Hazard ratio (95% CI)	P-value
Age (<50 vs. ≥50)	0.41 (0.26-0.66)	0.0002
Karnofsky performance score (≥70 vs. <70)	0.69 (0.47-1.00)	0.0607
MGMT expression (negative vs. positive)	0.59 (0.41-0.88)	0.0081
Extent of resection (≥90 vs. <90)	0.60 (0.39-0.93)	0.0211

Figure 2. Immunohistochemical analyses for MGMT expression. The representative cases for positive (A, B and C) and negative (D, E and F) immunostaining. The cut-off point for positive MGMT expression was set at 10%.

the statistical significance of the differences between patient characteristics of the two groups. Cox's proportional hazard model was used to analyze the prognostic variables. The hazard ratios for death were calculated considering adjustment for age, Karnofsky performance status score and the extent of resection.

Results

Efficacy of individualized chemotherapy. All specimens from the 74 patients were examined for their *in vitro* susceptibility to the 25 anticancer drugs. In this series of newly diagnosed glioblastoma patients, the success rate of the DST was 100%. There was remarkable heterogeneity in the most effective drug. The median survival time of all of the 74 glioblastoma patients treated with the individualized chemotherapy was 19.4 months (95% CI, 15.9-22.1), and the 2-year survival rate was 36.5% (95% CI, 24.3-48.7). The median progression-free survival was 9.2 months (95% CI, 7.6-12.3) (Fig. 1). The survival periods could be favorably compared with those treated with temozolomide, the present-day standard regimen for glioblastoma.

The univariate analysis showed that the clinical factors previously known to affect the survival of patients with glioblastoma were correlated with favorable prognosis in this study; a Karnofsky performance status score of ≥70%, tumor resection of ≥90% and <50 years of age. The multivariate analysis showed that <50 years of age and tumor resection of
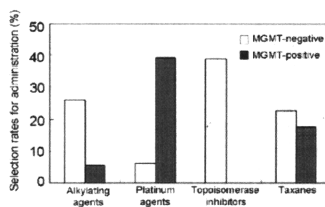

Figure 3. Selection rates of each anticancer drug as a key drug for administration; comparisons between the MGMT-negative and -positive glioblastomas.

≥90% were significantly associated with favorable prognosis (Table II, p=0.0002 and p=0.0211, respectively).

MGMT expression and chemosensitivity. The MGMT-positive rate was 53.7% for the 74 glioblastomas (Fig. 2). According to the DST, 58 tumors (78%) had at least one effective drug, and the other 16 tumors (22%) were negative for all of the 25 anticancer drugs examined (all-drug-resistant tumors). The relationship between the MGMT expression status and chemosensitivity was analyzed (Fig. 3). For the MGMT-positive tumors, the alkylating agents were selected only in two cases, and the topoisomerase inhibitors were never selected for administration as a key drug. The platinum agents were
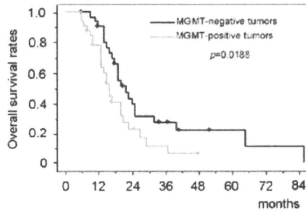
Figure 4. Kaplan-Meier analyses of the overall survival compared between MGMT-negative and MGMT-positive glioblastoma patients treated with individualized chemotherapy.
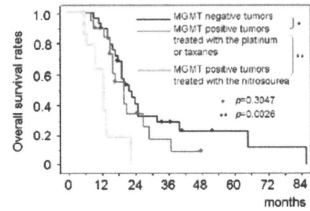

Figure 5. Kaplan-Meier analyses of the overall patient survival compared among MGMT-negative glioblastoma, MGMT-positive tumors treated with nitrosoureas and those treated with the platinum agents or the taxanes.

more frequently effective against the MGMT-positive tumors than against the MGMT-negative tumors. The taxanes were equally selected either in the MGMT-negative or the MGMT-positive group. Most of the all-drug-resistant tumors (14 out of 16 cases, 87.5%) were included in the MGMT-positive group (p=0.0019). Thus, the MGMT expression status significantly influenced the *in vitro* chemosensitivity of almost all categories of anticancer agents except for the taxanes.

MGMT expression and survival. The patients with negative MGMT immunostaining had significantly longer survival than those with positive MGMT [median survival, 22.3 months (95% CI, 17.6-27.0) vs. 15.1 months (95% CI, 13.4-16.8); p=0.0188] (Fig. 4). Immunohistochemical MGMT expression status had a significant impact on the survival period in the multivariate analysis (Table II). The survival period of the patients with MGMT-positive tumors treated with the platinum agents or the taxanes [median survival, 20.1 months (95% CI, 18.0-22.7)] was equivalent to that of the MGMT-negative tumors (p=0.3047) (Fig. 5). In contrast, the survival time of the patients with all-drug-resistant MGMT-positive tumors (n=14) who were treated with the nitrosourea-based chemotherapy (the modified PCV therapy) [median survival, 13.0 months (95% CI, 11.4-14.6)] was significantly shorter than both that of the patients with MGMT-negative tumors (p=0.0007) and that of MGMT-positive tumors treated with the platinum agents or the taxanes (p=0.0026).

Safety evaluation. We monitored the adverse events, with special focus on the hematological toxic effects. They were graded according to the National Cancer Institute's Common Toxicity Criteria version 3.0. Grade 3 or 4 neutropenia was observed in 9 patients (12.2%), and severe pneumonia occurred in 3 patients (4.1%). However, there was no treatment-related death in the present series.

Discussion

Our results suggest that individualized chemotherapy with anticancer drugs prospectively selected based on *in vitro* chemosensitivity tests for each glioblastoma patient provides a median survival of 19.4 months which compares favorably with most of the previously reported studies (2-4). The potentially poor prognosis groups with age greater than

50 years, Karnofsky performance status score less than 70% and surgical resection less than 90% particularly benefited from the individualized chemotherapy. Therefore, this study suggests an important new direction in the chemotherapy for glioblastoma.

An important implication of this study is that a large number of MGMT-positive glioblastomas were effectively treated with individualized chemotherapy. Many studies have indicated that MGMT is a significant prognostic factor for shorter survival rates in glioblastoma patients (5-7), whereas its prognostic value remains controversial (8,9). Efficacy of temozolomide also depends significantly on the level of MGMT expression (5). Therefore, one of the most important issues in contemporary neurooncology is how to treat glioblastoma with high MGMT expression. Therapeutic strategies for MGMT-positive glioblastoma currently under consideration have been designed to deplete MGMT and to combine other agents which are not affected by MGMT (21). The present results demonstrate that currently available anticancer drugs are much more effective when administered to those most likely to respond. An individualized or tailored strategy based on multiple biological information of the tumor would be one of the effective approaches to treat MGMT-positive glioblastoma.

However, an individualization strategy cannot easily be adopted in every institution. The lessons learned from individualized chemotherapy may be valuable in planning chemotherapy regimens for MGMT-positive glioblastoma. The present study suggests that the platinum agents and the taxanes can potentially prolong the survival of patients with MGMT-positive glioblastoma. The platinum agents as well as temozolomide and O^6-benzylguanine can abrogate MGMT activity (22). Several studies have also shown that the antitumor activity of platinum agents is not affected by MGMT activity (23-25). This knowledge has led to Phase II clinical trials with promising results (26-28). Although MGMT affected the efficacies of diverse anticancer drugs, only the taxanes were independent from the MGMT status. Taxanes were clinically used in some trials without marked improvement in the efficacy for glioblastoma (29-31). However, multiple molecular mechanisms were reported to affect their efficacies for glioma cells (32). It is preferable to treat MGMT-positive glioblastoma with multi-modality regimens including platinum agents or the taxanes.

Currently, MGMT expression is estimated mainly by methylation-specific PCR or immunohistochemistry (5-9). Methylation-specific PCR is highly sensitive but is unable to assess intratumoral heterogeneity and contaminating normal cells such as endothelial cells (8,9). A methylated band is observed even when cells that carry MGMT promoter hypermethylation represent only a minor portion of the tumor. Regulation of MGMT expression is a more complex phenomenon in which abnormal promoter methylation is not the sole determining factor. We employed immunohistochemistry to directly evaluate the final functional molecule and the intratumoral heterogeneity, although an objective threshold for evaluation may not be easily set. We used a cut-off value of 10%, whereas the reported values vary from 5 to 35% (8,9,33,34). The results showed a tendency of polarization of the MGMT-positive rate in the tumors with rates of less than 5% and those with more than 35%. Consequently, the overall positive rate in our study is consistent with published reports employing immunohistochemistry.

This is the first report to show that individualization of chemotherapy can potentially prolong the survival of non-selected consecutive glioblastoma patients with high MGMT expression without any additional toxicity. When the stratification based on the MGMT expression is available, platinum agents or the taxanes offer the highest probability for effectiveness against MGMT-positive glioblastomas.

References

1. Shapiro WR: Current therapy for brain tumors: back to the future. Arch Neurol 56: 429-432, 1999.
2. Medical Research Council Brain Tumor Working Party: Randomized trial of procarbazine, lomustine and vincristine in the adjuvant treatment of high-grade astrocytoma: a Medical Research Council trial. J Clin Oncol 19: 509-518, 2001.
3. Glioma Meta-analysis Trialist (GMT) Group: Chemotherapy in adult high-grade glioma: a systematic review and meta-analysis of individual patient data from 12 randomised trials. Lancet 359: 1011-1018, 2002.
4. Stupp R, Mason WP, van den Bent MJ, et al: European Organisation for Research and Treatment of Cancer Brain Tumor and Radiotherapy Groups; National Cancer Institute of Canada Clinical Trials Group: Radiotherapy plus concomitant and adjuvant temozolomide for glioblastoma. N Engl J Med 352: 987-996, 2005.
5. Hegi ME, Diserens AC, Gorlia T, et al: MGMT gene silencing and benefit from temozolomide in glioblastoma. N Engl J Med 352: 997-1003, 2005.
6. Jaeckle KA, Eyre HJ, Townsend JJ, et al: Correlation of tumor O⁶-alkylguanine-DNA methyltransferase levels with survival of malignant astrocytoma patients treated with bis-chloroethylnitrosourea: a Southwest Oncology Group study. J Clin Oncol 16: 3310-3315, 1998.
7. Esteller M, Garcia-Foncillas J, Andion E, et al: Inactivation of the DNA-repair gene MGMT and the clinical response of gliomas to alkylating agents. N Engl J Med 343: 1350-1354, 2000.
8. Brell M, Tortosa A, Verger E, et al: Prognostic significance of O⁶-alkylguanine-DNA methyltransferase determined by promoter hypermethylation and immunohistochemical expression in anaplastic gliomas. Clin Cancer Res 11: 5167-5174, 2005.
9. Chinot OL, Barrie M, Fuentes S, et al: Correlation between O⁶-alkylguanine-DNA methyltransferase and survival in inoperable newly diagnosed glioblastoma patients treated with neoadjuvant temozolomide. J Clin Oncol 25: 1470-1475, 2007.
10. Cortazar P and Johnson BE: Review of the efficacy of individualized chemotherapy selected by in vitro drug sensitivity testing for patients with cancer. J Clin Oncol 17: 1625-1631, 1999.
11. Alonso C: Human tumor stem cell assay. A prospective clinical trial. Cancer 54: 2475-2479, 1984.
12. Von Hoff DD, Sandbach JF, Clark GM, et al: Selection of cancer chemotherapy for a patient by an in vitro assay versus a clinician. J Natl Cancer Inst 82: 110-116, 1990.
13. Gazdar AF, Steinberg SM, Russell EK, et al: Correlation of in vitro drug-sensitivity testing with response to chemotherapy and survival in extensive-stage small cell lung cancer: a prospective clinical trial. J Natl Cancer Inst 82: 117-124, 1990.
14. Cortazar P, Gazdar AF, Woods E, et al: Survival of patients with limited-stage small cell lung cancer treated with individualized chemotherapy selected by in vitro drug sensitivity testing. Clin Cancer Res 3: 741-747, 1997.
15. Iwadate Y, Fujimoto S, Namba H and Yamaura A: Promising survival for patients with glioblastoma multiforme treated with individualised chemotherapy based on in vitro drug sensitivity testing. Br J Cancer 89: 1896-1900, 2003.
16. Iwadate Y, Fujimoto S, Sueyoshi K, et al: Prediction of drug cytotoxicity in 9L rat brain tumor by using flow cytometry with a deoxyribonucleic acid-binding dye. Neurosurgery 40: 782-788, 1997.
17. Iwadate Y, Fujimoto S and Yamaura A: Differential chemosensitivity in human intracerebral gliomas measured by flow cytometric DNA analysis. Int J Mol Med 10: 187-192, 2002.
18. Alberts DS and Chen HSG: Tabular Summary of Pharmacokinetic Parameters Relevant to In Vitro Drug Assay. Alan R. Liss, New York, pp351-359, 1980.
19. Higuchi Y, Iwadate Y and Yamaura A: Treatment of low-grade oligodendroglial tumors without radiotherapy. Neurology 63: 2384-2386, 2004.
20. Iwadate Y, Namba H and Sueyoshi K: Intra-arterial ACNU and cisplatin chemotherapy for the treatment of glioblastoma multiforme. Neurol Med Chir 35: 598-603, 1995.
21. Mason WP and Cairncross JG: Drug insight: temozolomide as a treatment for malignant glioma – impact of a recent trial. Nat Clin Pract Neurol 1: 88-95, 2005.
22. Tanaka S, Kobayashi I, Utsuki S, Oka H, Yasui Y and Fujii K: Down-regulation of O⁶-methylguanine-DNA methyltransferase gene expression in gliomas by platinum compounds. Oncol Rep 14: 1275-1280, 2005.
23. Beith J, Hartley J, Darling J and Souhami R: DNA interstrand cross-linking and cytotoxicity induced by chloroethylnitrosoureas and cisplatin in human glioblastoma cell lines which vary in cellular concentration of O⁶-alkylguanine-DNA methyltransferase. Br J Cancer 75: 500-505, 1997.
24. Preuss I, Thust R and Kaina B: Protective effect of O⁶-methylguanine-DNA methyltransferase (MGMT) on the cytotoxic and recombinigenic activity of different antineoplastic drugs. Int J Cancer 65: 506-512, 1996.
25. Fruehauf JP, Brem H, Parker R, et al: In vitro drug response and molecular markers associated with drug resistance in malignant gliomas. Clin Cancer Res 12: 4523-4532, 2006.
26. Balana C, Ramirez JL, Rosell R, et al: O⁶-methylguanine-DNA methyltransferase methylation in serum and tumor DNA predicts response to 1,3-bis(2-chloroethyl)-1-nitrosourea but not to temozolomide plus cisplatin in glioblastoma multiforme. Clin Cancer Res 9: 1461-1468, 2003.
27. Watanabe T, Katayama Y, Ogino A, et al: Preliminary individualized chemotherapy for malignant astrocytomas based on O⁶-methylguanine-deoxyribonucleic acid methyltransferase methylation analysis. Neurol Med Chir 46: 387-394, 2006.
28. Silvani A, Eoli M, Salmaggi A, et al: Phase II trial of cisplatin plus temozolomide, in recurrent and progressive malignant glioma patients. J Neurooncol 66: 203-208, 2004.
29. Rosenthal MA, Gruber ML, Glass J, et al: Phase II study of combination taxol and estramustine phosphate in the treatment of recurrent glioblastoma multiforme. J Neurooncol 47: 59-63, 2000.
30. Langer CJ, Ruffer J, Rhodes H, et al: Phase II Radiation Therapy Oncology Group trial of weekly paclitaxel and conventional external beam radiation therapy for supratentorial glioblastoma multiforme. Int J Radiat Oncol Biol Phys 51: 113-119, 2001.
31. Ashamalla H, Zaki B, Mokhtar B, et al: Fractionated stereotactic radiotherapy boost and weekly paclitaxel in malignant gliomas clinical and pharmacokinetics results. Technol Cancer Res Treat 6: 169-176, 2007.
32. Karmakar S, Banik NL and Ray SK: Combination of all-trans retinoic acid and paclitaxel-induced differentiation and apoptosis in human glioblastoma U87MG xenografts in nude mice. Cancer 112: 596-607, 2008.
33. Friedman HS, McLendon RE, Kerby T, et al: DNA mismatch repair and O⁶-alkylguanine-DNA alkyltransferase analysis and response to Temodal in newly diagnosed malignant glioma. J Clin Oncol 16: 3851-3857, 1998.
34. Mollemann M, Wolter M, Felsberg J, et al: Frequent promoter hypermethylation and low expression of the MGMT gene in oligodendroglial tumors. Int J Cancer 113: 379-385, 2005.

CLINICAL STUDY – PATIENT STUDY

Favorable long-term outcome of low-grade oligodendrogliomas irrespective of 1p/19q status when treated without radiotherapy

Yasuo Iwadate · Tomoo Matsutani ·
Yuzo Hasegawa · Natsuki Shinozaki ·
Yoshinori Higuchi · Naokatsu Saeki

Abstract Despite the accumulating evidences of high chemosensitivity especially in anaplastic oligodendrogliomas with loss of chromosomes 1p and 19q, the optimal management strategy for low-grade tumors using the 1p/19q information remains controversial. We have treated all low-grade oligodendrogliomas by a chemotherapy-preceding strategy without radiotherapy, and here we analyzed the survival outcomes of 36 consecutive patients in relation to 1p/19q status. The treatment protocol was as follows: (1) simple observation after gross total resection, and (2) modified PCV chemotherapy for postoperative residual tumors or recurrence after total resection. The 1p and 19q status were analyzed by fluorescence in situ hybridization. The median follow-up period was 7.5 years and no patient was lost during the follow-up periods. 1p/19q co-deletion was observed in 72% of the patients, and there was no significant association between 1p/19q co-deletion and chemotherapy response rate. The 5- and 10-year progression-free survival (PFS) rate was 75.1 and 46.9%, respectively, and the median PFS was 121 months for 1p/19q-deleted tumors and 101 months for non-deleted tumors (log-rank test: $P = 0.894$). Extent of surgery did not affect PFS ($P = 0.685$). In contrast, the elder patients (>50) had significantly shorter PFS ($P = 0.0458$). Recurrent tumors were well controlled by chemotherapy irrespective of 1p/19q status, and 35 out of 36 patients survived without receiving radiotherapy. The 5- and 10-year overall survival rates were 100 and 93.8%, respectively. Two of the patients in their sixties (29%) suffered from severe cognitive dysfunctions and marked brain atrophy following chemotherapy alone. These results show that low-grade oligodendrogliomas could be successfully treated by surgical resection and nitrosourea-based chemotherapy alone without radiotherapy irrespective of 1p/19q status.

Keywords 1p/19q · Chemotherapy · Leukoencephalopathy · Neurotoxicity · Oligodendroglial tumor · PCV

Introduction

The therapeutic strategy for adult low-grade gliomas, especially as regards the choice and timing of radiotherapy, is still controversial [1–4]. Although radiotherapy is undoubtedly beneficial for a subset of patients with low-grade gliomas, the natural history of gliomas when not irradiated after surgery is largely unknown. Only four prospective randomized trials have been conducted regarding the efficacy of radiotherapy for low-grade gliomas, and none of them could demonstrate any significant benefits on overall survival (OS). The EORTC 22845 randomized trial suggested that immediate postoperative radiotherapy for any residual tumors has advantages in terms of progression-free survival (PFS) but not in terms of OS [1, 3]. On the other hand, radiation-induced toxicities such as delayed cognitive dysfunction and leukoencephalopathy are important factors to determine treatment strategy [5, 6].

Stratification or personalization of the treatment strategy based on some markers is expected. Among gliomas, deletions of chromosomes 1p and 19q are shown to be associated with tumors including oligodendroglial components [7]. The co-deletion has also been associated with

Y. Iwadate (✉) · T. Matsutani · Y. Hasegawa · N. Shinozaki ·
Y. Higuchi · N. Saeki
Department of Neurological Surgery,
Chiba University Graduate School of Medicine,
1-8-1 Inohana, Chuo-ku, Chiba 260-8670, Japan
e-mail: iwadatey@faculty.chiba-u.jp

🖄 Springer

responsiveness of anaplastic oligodendroglial tumors to radiotherapy and chemotherapy as well as with prolonged survival of the patients [8, 9]. However, this predictive and prognostic relevance of the 1p/19q co-deletion are more controversial for low-grade tumors [10–17]. To elucidate this issue, a long follow-up period is necessary because the patients with low-grade oligodendroglial tumors usually have more favorable outcome than anaplastic tumors.

In addition to the controversy in the application of radiotherapy, it has been reported that low-grade oligodendroglial tumors respond well to chemotherapy [18–21]. Therefore, we have treated all patients without using radiotherapy and have applied a nitrosourea-based chemotherapy (PAV, a modified PCV) when postoperative progressing tumors were verified [19]. The aim of this study was to elucidate the long-term outcome of low-grade oligodendrogliomas treated with chemotherapy-preceding strategy without radiotherapy in relation to 1p/19q co-deletion.

Methods

Patients and treatment

Since 1995, we have prospectively treated all patients having low-grade oligodendrogliomas by a radiotherapy-deferring and chemotherapy-preceding strategy using a standard nitrosourea-based chemotherapy (PAV, a modified PCV). The classic oligodendroglioma histological features were defined by areas composed of uniform and round nuclei surrounded by perinuclear halos and in an even tissue distribution [15]. The treatment protocol was: (1) simple observation after complete resection of tumors, and (2) PAV for postoperative residual tumors or recurrence after total resection. In this chemotherapy, lomustine (CCNU) was replaced with nimustine (ACNU; [1-(4-amino-2-methyl-5-pyrimidinyl)-methyl-(2-chloroethyl)-3-nitrosourea hydrochloride] which is a water- and lipid-soluble nitrosourea derivative. The chemotherapy protocol was ACNU 75 mg/m^2 on day 1, vincristine 1 mg/m^2 on days 8 and 29, and procarbazine 100 mg/day on days 8–21; this cycle was administered four times a year for 2 years [19]. Patients were required to provide written informed consent before receiving the chemotherapy.

Data collection

All patients histologically confirmed to have oligodendroglioma or oligoastrocytoma were enrolled in this study. Age, sex, tumor location, tumor size, pathological diagnosis, and extents of resection were recorded. None of the patients was excluded from analysis because of early

recurrence within 1 year after surgery. Magnetic resonance imaging (MRI) studies were performed preoperatively, postoperatively within 2 weeks, and after every course of chemotherapy. Tumor volume was estimated as the product of the three largest perpendicular diameters of all measurable lesions on fluid-attenuated inversion recovery (FLAIR) with reference to pre- and postgadolinium T1-weighted MRI. Regarding the extent of surgery, gross total resection was defined as a disappearance of the tumor on MRI, and subtotal resection as a ≥70% reduction of the tumor size. Responses to chemotherapy were determined in the patients with postoperative residual tumors using the modified Macdonald criteria [22], in which complete response (CR) was defined as disappearance of all measurable disease, and partial response (PR) was defined as ≥50% decrease in the measured tumor size compared with baseline. Progressive disease (PD) was defined as ≥25% increase of the tumor size and stable disease (SD) was applied to all other situations. Toxicity was graded according to the National Cancer Institute's Common Toxicity Criteria version 3.0.

The histological diagnosis was confirmed by a neuropathologist other than the initial diagnostician. Chromosome 1p- and 19q-deletion analyses were done using a standard fluorescence in situ hybridization (FISH) of fixed cytogenetic preparation from fresh tumor tissues [23]. FISH probes for 1p were the target region of 1p36 with a control region of 1q25, and those for 19q were the control region of 19p13 with the target region of 19q13. The total number of signals was counted, and the ratio of 1p:1q or 19q:19p of <0.75 was diagnosed as loss.

Statistical analysis

Progression-free survival was calculated from the date of diagnosis until the first sign of radiological progression, death, or last follow-up. OS was calculated from the date of diagnosis until the date of death or last follow-up. The Kaplan–Meier method was used to estimate survival rates and the log-rank test was applied to compare the survival differences using StatView software (SAS Institute, Cary, NC, USA). A Fisher exact test was performed to determine the association between 1p/19q co-deletion and chemotherapy response rate. Cox's proportional hazard regression model was used to perform multivariate analysis for the possible prognostic variables including age, extent of resection, 1p19q status (SPSS, Chicago, IL, USA).

Results

Thirty-six consecutive patients with histologically proven low-grade oligodendrogliomas were treated between 1995

Table 1 Patient characteristics

Age	
Mean	43
Range	22–68
>50	14 (39%)
Sex (%)	
Male	24 (67)
Female	12 (33)
Karnofsky performance score (%)	
≧70	35 (97)
<70	1 (3)
Histology (%)	
Oligodendroglioma	33 (92)
Oligoastrocytoma	3 (8)
1p/19q deletion (%)	
Yes	23 (72)
No	8 (22)
Extent of surgery (%)	
Gross total	15 (42)
Subtotal/partial	21 (58)
Chemotherapy (%)	
Yes	26 (72)
No	10 (28)
Recurrence (%)	
Yes	15 (42)
No	21 (58)

Fig. 1 Kaplan–Meier analyses for the progression-free survival of all 36 patients with low-grade oligodendrogliomas (a), and those comparing by extent of surgery (b) and age (c) are shown. *Tick marks* indicate last follow-up

and 2008 (Table 1). Thirty-three patients had oligodendrogliomas and three had oligoastrocytomas. There were 24 men and 12 women with a mean age of 43 years (range 22–68 years). The patients were followed up with for a median period of 7.5 years and no patient was lost during the follow-up period. Fifteen patients (42%) underwent gross total resection, 10 patients (28%) underwent subtotal tumor resection, and the other 11 (30%) underwent partial resection. Twenty-six patients were treated with chemotherapy. Tumor recurrence occurred in 15 patients (42%); 5 patients after total resection (5/15: 33%), 4 after subtotal resection (4/10: 40%), and 6 after partial resection (6/11: 55%).

The 5- and 10-year PFS rates were 75.1 and 46.9%, respectively, and the median PFS was 101 months (Fig. 1a). There was no significant difference of PFS between the patients who were observed after total resection and those with incomplete resection followed by the chemotherapy (median PFS, 121 vs 93 months, respectively, $P = 0.685$) (Fig. 1b). In contrast, the elder patients (>50) had significantly shorter PFS ($P = 0.0458$) (Fig. 1c). There was no difference in clinical course including PFS between the patients with oligodendroglioma and oligoastrocytoma. A salvage second surgery was performed in
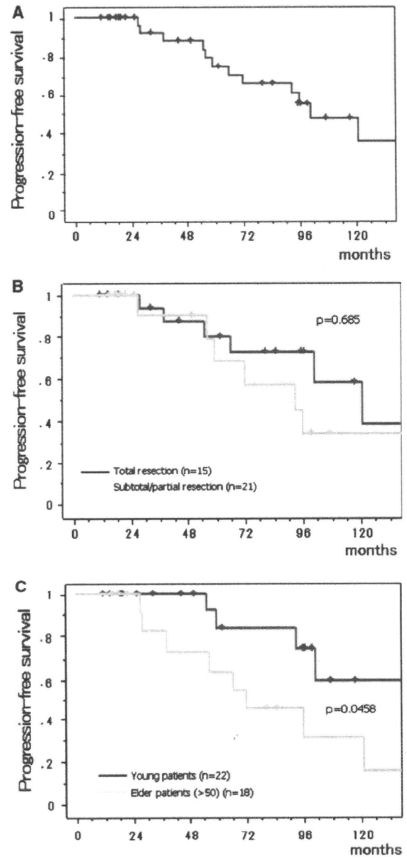
seven cases, and malignant transformation was not observed in the present non-irradiated series. There was a patient whose tumor had 1p/19q loss but finally could not be controlled by chemotherapy. This patient refused radiotherapy and died at 81 months after surgery. Therefore, no patient in the present study received radiotherapy, and 35 out of 36 patients survived without receiving
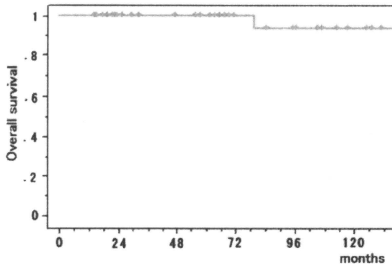
Fig. 2 Kaplan–Meier analyses for the overall survival of all 36 patients with low-grade oligodendrogliomas treated by surgical resection and chemotherapy without radiotherapy is shown. *Tick marks* indicate last follow-up
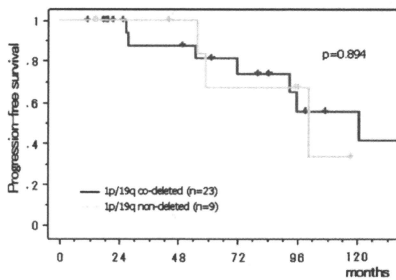
Fig. 3 Kaplan–Meier analyses for the progression-free survival of patients with low-grade oligodendrogliomas with and without 1p19q co-deletion are shown. *Tick marks* indicate last follow-up

radiotherapy at the follow-up period of 10 years; 5- and 10-year OS rates were 100 and 93.8%, respectively (Fig. 2).

1p/19q co-deletion was observed in 23 of 32 cases (72%) analyzed with FISH. Isolated loss of 1p or 19q was not observed in the present series. Median PFS rate for the patients with 1p/19q co-deleted tumors was 121 months and that for non-deleted tumors was 101 months. There was no significant difference in PFS between the patients with 1p/19q co-deleted tumors and those without co-deletion ($P = 0.894$) (Fig. 3). The multivariate analysis showed that neither of age, extent of resection, nor 1p/19q status were significantly associated with the length of PFS (Table 2).

Two patients in their sixties manifested marked brain atrophy without tumor recurrence 4–5 years after the initiation of chemotherapy (Fig. 4). These patients required intensive nursing care and observation because of their developing cognitive deficits. The MRI finding of tight high-convexity, which is typical for normal pressure

Table 2 Multivariate analyses for the possible prognostic factors

	P
Age (<50 vs ≥50)	0.1274
Extent of resection (total vs non-total)	0.7089
1p19q co-deletion (deleted vs non-deleted)	0.3995

hydrocephalus, was not observed and the CSF tap test was negative in the patients. A grade 3 or 4 leukopenia mandating a treatment delay occurred in two patients (9%).

Discussion

The present study showed that, when treated with a radiotherapy-deferring and chemotherapy-preceding strategy using modified PCV chemotherapy, the 10-year OS rates of low-grade oligodendrogliomas were over 90% irrespective of 1p/19q status. This outcome compares favorably with those of previous reports including immediate postoperative radiotherapy without chemotherapy; the median survival times were within 5.3–14.9 years [24–27, 31], and 5- and 10-year OS rates were 52–95% [24–31] and 24–85% [24, 25, 27–29, 31], respectively. The median times to tumor progression were within 5.6–13.2 years [26, 31], and the 5-year PFS rate was reported as 67% [30]. In addition, it was reported that neither PFS and OS were significantly improved by radiotherapy in retrospective studies employing chemotherapy [32–34]. As a new therapeutic strategy for low-grade oligodendrogliomas, the effectiveness of PCV chemotherapy has been reported [18–21, 35–38], and some authors have concluded that radiotherapy could be postponed until malignant transformation occurs [3, 18–21, 32, 35]. The present result is in accordance with these studies. In contrast, although PCV chemotherapy for low-grade oligodendrogliomas achieved stabilization or shrinkage of tumors, its efficacy was not curative in many cases, as shown by the increased recurrence rate at 10-year follow-up. A longer observation period in a larger cohort would be necessary to clarify the validity of the radiotherapy-deferring and chemotherapy-preceding strategy against low-grade oligodendrogliomas.

Since a subset of low-grade gliomas progresses to malignant tumors, some stratification or personalization in the treatment planning are expected. In addition to the diagnostic relevance for oligodendroglial tumors, the prognostic role of 1p/19q loss is well defined for anaplastic oligodendrogliomas [8, 9]. For grade III tumors, 1p/19q loss may characterize a less malignant variant of the tumor, and the gene products lost as a consequence of 1p/19q loss may be mediators of resistance to genotoxic therapies [14]. In contrast, the prognostic relevance is less defined for
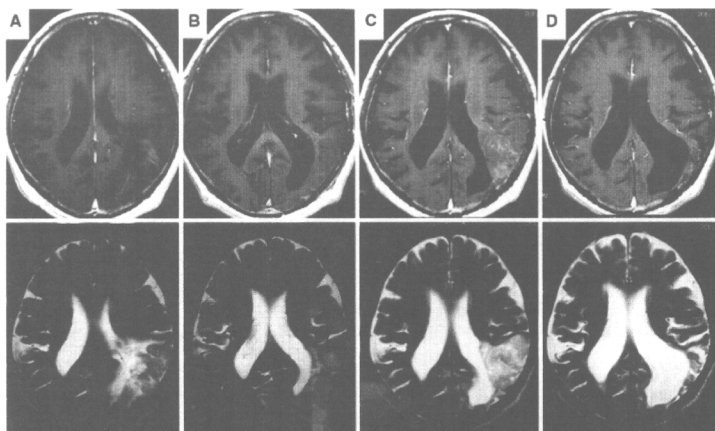
Fig. 4 The representative MRI pictures (*upper panel*; gadolinium-enhanced T1 weighted images, *lower*; T2-weighted images) of a patient aged 68 years. A left parietal tumor at initial diagnosis (**a**) was completely resected after surgery (**b**), and the tumor recurred 2.5 years after the surgery (**c**). Although chemotherapy with ACNU, vincristine and procarbazine achieved a complete response, the patient's neurological condition gradually worsened. Marked enlargement of the cortical sulci and lateral ventricles was observed without tumor recurrence at 7 years from diagnosis (**d**)

low-grade oligodendroglial tumors [10–17]. Our result showed that the outcome of patients with histologically typical low-grade oligodendrogliomas was generally favorable irrespective of 1p/19q status when treated without radiotherapy. Although 1p/19q loss is one of the major genetic alterations in oligodendroglial tumors [7, 23], other important genetic alterations would exist as an early event. The previous contradictory results may be partly due to heterogeneity in histology and treatments [10–17]. Radiotherapy would negatively modify the survival results of the patients having tumors without 1p/19q deletions [23]. However, the small sample size may have contributed to this result, and a future prospective study including more patients with 1p/19q information is needed.

Recently, temozolomide (TMZ) has been frequently used as the initial treatment for oligodendrogliomas with high response rates almost equivalent to those of PCV chemotherapy [10, 16]. Both of these chemotherapy regimens would be effective for low-grade oligodendrogliomas. TMZ is advantageous due to its safety profile especially with regard to hematologic toxicity. Standard 42-day PCV chemotherapy induces significant hematologic toxicity, requiring a dose reduction and/or a cycle delay [19, 36]. Therefore, we applied a prolonged-cycle interval schedule to avoid the cumulative hematologic toxicity of PAV, and the incidence rate of grade 3 or 4 leukopenia was acceptably low.

In the present study, the other adverse effect following the modified PAV chemotherapy was found after long-term observations. Two patients in their sixties underwent marked brain atrophy following chemotherapy without receiving radiotherapy. Other causes of brain atrophy due to aging, such as normal pressure hydrocephalus or multiple cerebral infarctions, could not be completely excluded. However, the MRI findings of tight high-convexity and the CSF tap test were both negative, and they had not had the risk factors for cerebral infarction. Although neurotoxicities of an intensive PCV regimen have been reported [38, 39], this is the first report of a potential neurotoxicity following a standard nitrosourea-based chemotherapy alone. This adverse effect could not be detected within short-term follow-up periods. Careful application of chemotherapy for patients older than 60 years is recommended. In contrast, the recurrence rate was higher in older patients than in younger patients, which highlighted the importance of surgical resection. Attempting the greatest possible surgical resection without neurological deteriorations followed by simple observation may be the best way to treat low-grade oligodendrogliomas, especially for the elder patients.

References

1. Karim AB, Afra D, Cornu P, Bleehan N, Schraub S, De Witte O, Darcel F, Stenning S, Pierart M, Van Glabbeke M (2002) Randomized trial on the efficacy of radiotherapy for cerebral low-grade gliomas in the adult: European Organization for Research and Treatment of Cancer Study 22845 with Medical Research Council Study BRO4: an interim analysis. Int J Radiat Oncol Biol Phys 52:316–324
2. Shaw E, Arusell R, Scheithauer B et al (2002) Prospective randomized trial of low- versus high-dose radiation therapy in adults with supratentorial low-grade glioma: initial report of a North Central Cancer Treatment Group/Radiation Therapy Oncology Group/Eastern Cooperative Group study. J Clin Oncol 20:2267–2276
3. van den Bent MJ, Afra D, de Witte O, Ben Hassel M, Schraub S, Hoang-Xuan K, Malmström PO, Collette L, Piérart M, Mirimanoff R, Karim AB, EORTC Radiotherapy and Brain Tumor Groups and the UK Medical Research Council (2005) Long-term efficacy of early versus delayed radiotherapy for low-grade astrocytoma and oligodendroglioma in adults: the EORTC 22845 randomised trial. Lancet 366:985–990
4. Papagikos MA, Shaw EG, Stieber VW (2005) Lessons from randomized clinical trials in adult low grade glioma. Lancet Oncol 6:240–244
5. Behin A, Hoang-Xuan K, Carpentier AF, Delattre J-Y (2003) Primary brain tumors in adults. Lancet 361:323–331
6. Wessels PH, Weber WE, Raven G, Ramaekers FC, Hopman AH, Twijnstra A (2003) Supratentorial grade II astrocytoma: biological features and clinical course. Lancet Neurol 2: 395–403
7. Bello MJ, Vaquero J, de Campos JM, Kusak ME, Sarasa JL, Saez-Castresana J, Pestana A, Rey JA (1994) Molecular analysis of chromosome 1 abnormalities in human gliomas reveals frequent loss of 1p in oligodendroglial tumors. Int J Cancer 57: 172–175
8. Caincross G, Berkey B, Shaw E et al (2006) Phase III trial of chemotherapy plus radiotherapy compared with radiotherapy alone for pure and mixed anaplastic oligodendroglioma: Intergroup Radiation Therapy Oncology Group Trial 9402. J Clin Oncol 24:2707–2714
9. van den Bent MJ, Carpentier AF, Brandes AA et al (2006) Adjuvant procarbazine, lomustine, and vincristine improves progression-free survival but not overall survival in newly diagnosed anaplastic oligodendrogliomas and oligoastrocytomas: a randomized European Organization for Research and Treatment of Cancer phase III trial. J Clin Oncol 24:2715–2722
10. Hoang-Xuan K, Capelle L, Kujas M et al (2004) Temozolomide as initial treatment for adults with low-grade oligodendrogliomas or oligoastrocytomas and correlation with chromosome 1p deletions. J Clin Oncol 22:3133–3138
11. Kanner AA, Staugaitis SM, Castilla EA et al (2006) The impact of genotype on outcome in oligodendroglioma: validation of the loss of chromosome arm 1p as an important factor in clinical decision making. J Neurosurg 104:542–550
12. Mariani L, Deiana G, Vassella E, Fathi AR, Murtin C, Arnold M, Vajtai I, Weis J, Siegenthaler P, Schobesberger M, Reinert MM (2006) Loss of heterozygosity 1p36 and 19q13 is a prognostic factor for overall survival in patients with diffuse WHO grade 2 gliomas treated without chemotherapy. J Clin Oncol 24: 4758–4763
13. Jaeckle KA, Ballman KV, Rao RD, Jenkins RB, Buckner JC (2006) Current strategies in treatment of oligodendroglioma: evolution of molecular signature of response. J Clin Oncol 24:1246–1252

14. Weller M, Berger H, Hartmann C et al (2007) Combined 1p/19q loss in oligodendroglial tumors: predictive or prognostic biomarker? Clin Cancer Res 13:6933–6937
15. Giannini C, Burger PC, Berkey BA, Cairncross JG, Jenkins RB, Mehta M, Curran WJ, Aldape K (2008) Anaplastic oligodendroglial tumors: refining the correlation among histopathology, 1p 19q deletion and clinical outcome in Intergroup Radiation Therapy Oncology Group Trial 9402. Brain Pathol 18:360–369
16. Kaloshi G, Benouaich-Amiel A, Diakite F et al (2007) Temozolomide for low-grade gliomas. Predictive impact of 1p/19q loss on response and outcome. Neurology 68:1831–1836
17. Capelle L, Oei P, Teoh H, Hamilton D, Palmer D, Low I, Campbell G (2009) Retrospective review of prognostic factors, including 1p19q deletion, in low-grade oligodendrogliomas and a review of recent published works. J Med Imaging Radiat Oncol 53:305–309
18. Mason WP, Krol GS, DeAngelis LM (1996) Low-grade oligodendrogliomas respond to chemotherapy. Neurology 46:203–207
19. Higuchi Y, Iwadate Y, Yamaura A (2004) Treatment of low-grade oligodendroglial tumors without radiotherapy. Neurology 63:2384–2386
20. Sunyach MP, Jouvet A, Perol D, Jouanneau E, Guyotat J, Gignoux L, Carrie C, Frappaz D (2007) Role of exclusive chemotherapy as first line treatment in oligodendroglioma. J Neurooncol 85:319–328
21. Bromberg JEC, van den Bent MJ (2009) Oligodendrogliomas: molecular biology and treatment. Oncologist 14:155–163
22. Macdonald DR, Cascino TL, Schold SC Jr, Cairncross JG (1990) Response criteria for phase II studies of supratentorial malignant glioma. J Clin Oncol 8:1277–1280
23. Jenkins RB, Blair H, Ballman KV et al (2006) A t(1;19)(q10;p10) mediates the combined deletions of 1p and 19q and predicts a better prognosis of patients with oligodendroglioma. Cancer Res 66:9852–9861
24. Shaw EG, Scheithauser BW, O'Fallon JR, Tazellar HD, Davis DH (1992) Oligodendrogliomas: the Mayo Clinic experience. J Neurosurg 76:428–434
25. Celli P, Nofrone I, Palma L, Cantore G, Fortuna A (1994) Cerebral oligodendroglioma: prognostic factors and life history. Neurosurgery 35:1018–1034
26. Leighton C, Fisher B, Bauman G, Depiero S, Stitt L, MacDonald D, Cairncross G (1997) Supratentorial low-grade glioma in adults: an analysis of prognostic factors and timing of radiation. J Clin Oncol 15:1294–1301
27. Leonardi MA, Lumenta CB (2001) Oligodendrogliomas in CT/MR-era. Acta Neurochir 143:1195–1203
28. Okamoto Y, Di Patre OL, Birkhard C et al (2004) Population-based study on incidence, survival rates, and genetic alterations of low-grade diffuse astrocytomas and oligodendrogliomas. Acta Neuropathol 108:49–56
29. Lebrun C, Fontaine D, Ramaioli A, Vandenbos F, Chanalet S, Lonjon M, Michiels JF, Bourg V, Paquis P, Chatel M, Frenay M, Nice Brain Tumor Study Group (2004) Long-term outcome of oligodendrogliomas. Neurology 62:1783–1787
30. Yeh SA, Lee TC, Chen HJ, Lui CC, Sun LM, Wang CJ, Huang EY (2002) Treatment outcome and prognostic factors in patients with supratentorial low-grade oligodendrogliomas. Int J Radiat Oncol Biol Phys 54:1405–1409
31. Kang H-C, Kim IH, Eom K-Y, Kim JH, Jung H-W (2009) The role of radiotherapy in the treatment of newly diagnosed supratentorial low-grade oligodendrogliomas: comparative analysis with immediate radiotherapy versus surgery alone. Cancer Res Treat 41:132–137
32. Olson JD, Riedel E, DeAngelis LM (2000) Long-term outcome of low-grade oligodendroglioma and mixed glioma. Neurology 54:1442–1448

33. Ozyigit G, Onal C, Gurkaynak M, Soylemezoklu F, Zorlu F (2005) Postoperative radiotherapy and chemotherapy in the management of oligodendroglioma: single institutional review of 88 patients. J Neurooncol 75:189–193

34. El-Hatter H, Souhami L, Roberge D, Del Maestro R, Leblanc R, Eldebawy E, Muanza T, Melancon D, Kavan P, Guiot MC (2009) Low-grade oligodendroglioma: an indolent but incurable disease? J Neurosurg 111:265–271

35. Stege EM, Kros JM, de Bruin HG, Enting RH, van Heuvel I, Looijenga LH, van der Rijt CD, Smitt PA, van den Bent MJ (2005) Successful treatment of low-grade oligodendroglial tumors with a chemotherapy regimen of procarbazine, lomustine, and vincristine. Cancer 103:802–809

36. Ty AU, See SJ, Rao JP, Khoo JB, Wong MC (2006) Oligodendroglial tumor chemotherapy using "decreased-dose-intensity" PCV: a Singapore experience. Neurology 66:247–249

37. Lebrun C, Fontaine D, Bourg V, Ramaioli A, Chanalet S, Vandenbos F, Lonjon M, Fauchon F, Paquis P, Frenay M (2007) Treatment of newly diagnosed symptomatic pure low-grade oligodendrogliomas with PCV chemotherapy. Eur J Neurol 14:391–398

38. Buckner JC, Geame D, O'Fallon JR et al (2003) Phase II trial of patients with low grade oligodendroglioma and oligoastrocytoma: efficacy and associations with chromosomal abnormalities. J Clin Oncol 21:251–255

39. Postma TJ, van Groeningen CJ, Witjes RJ, Weerts JG, Kralendonk JH, Heimans JJ (1998) Neurotoxicity of combination chemotherapy with procarbazine, CCNU and vincristine (PCV) for recurrent glioma. J Neurooncol 38:69–75

Urokinase-Targeted Fusion by Oncolytic Sendai Virus Eradicates Orthotopic Glioblastomas by Pronounced Synergy With Interferon-β Gene

Yuzo Hasegawa[1], Hiroaki Kinoh[2], Yasuo Iwadate[3], Mitsuho Onimaru[3], Yasuji Ueda[2], Yui Harada[4], Satoru Saito[4], Aki Furuya[4], Takashi Saegusa[5], Yosuke Morodomi[4,6], Mamoru Hasegawa[2], Shigeyoshi Saito[7], Ichio Aoki[7], Naokatsu Saeki[1] and Yoshikazu Yonemitsu[4]

[1]Department of Neurological Surgery, Chiba University Graduate School of Medicine, Chiba, Japan; [2]DNAVEC Corporation, Tsukuba, Japan; [3]Department of Pathology, Graduate School of Medical Sciences, Kyushu University, Fukuoka, Japan; [4]R&D Laboratory for Innovative Biotherapeutics, Graduate School of Pharmaceutical Sciences, Kyushu University, Fukuoka, Japan; [5]Department of Neurological Surgery, Chiba Rosai Hospital, Chiba, Japan; [6]Department of Surgery and Science, Graduate School of Medical Sciences, Kyushu University, Fukuoka, Japan; [7]Molecular Imaging Center, National Institute of Radiological Sciences, Chiba, Japan

Glioblastoma multiforme (GM), the most frequent primary malignant brain tumor, is highly invasive due to the expression of proteases, including urokinase-type plasminogen activator (uPA). Here, we show the potential of our new and powerful recombinant Sendai virus (rSeV) showing uPA-specific cell-to-cell fusion activity [rSeV/dMFct14 (uPA2), named "BioKnife"] for GM treatment, an effect that was synergistically enhanced by arming BioKnife with the interferon-β (IFN-β) gene. BioKnife killed human GM cell lines efficiently in a uPA-dependent fashion, and this killing was prevented by PA inhibitor-1. Rat gliosarcoma 9L cells expressing both uPA and its functional receptor uPAR (9L-L/R) exhibited high uPA activity on the cellular surface and were highly susceptible to BioKnife. Although parent 9L cells (9L-P) were resistant to BioKnife and to BioKnife expressing IFN-β (BioKnife-IFNβ), cell–cell fusion of 9L-L/R strongly facilitated the expression of IFN-β, and in turn, IFN-β significantly accelerated the fusion activity of BioKnife. A similar synergy was seen in a rat orthotopic brain GM model with 9L-L/R *in vivo*; therefore, these results suggest that BioKnife-IFNβ may have significant potential to improve the survival of GM patients in a clinical setting.

INTRODUCTION

Glioblastoma multiforme (GM), the most frequent primary malignant brain tumor, is highly invasive and intractable, and the median survival of patients bearing GM is merely 1 year with current standard treatments, including surgery and radiotherapy.[1] A recent clinical trial revealed that temozolomide, an oral alkylating agent, achieved significant improvement of the median survival of patients of GM to 14.6 months;[2] however, another

study reported that 73.5% of patients still die within <2 years and 72.2% experience recurrence.[3] The highly invasive nature of GM is a cause of great frustration among surgeons and is responsible for the high rate of local recurrence; extended resection for complete removal of tumor cells is usually difficult without injuring surrounding brain tissues, and therefore, the surgical margin is frequently regarded as positive.

There is thus an urgent need for new approaches in GM treatment. Virus-based therapeutics for glioblastoma have been evaluated in clinical studies over the last decade, including a packaging cell-mediated local production of retroviruses expressing herpes simplex virus thymidine kinase.[4] Even though these viruses have been shown to increase oncolytic activity and tumor specificity, no significant therapeutic effects have been reported in the clinical trials to date;[5] therefore, researchers are focusing their current efforts on improving new viruses that target GM[6–9] including a unique oncolytic adenovirus that targets mutant variant III of the epithelial growth factor receptor (EGFRvIII), which is a glioblastoma-specific mutant. In our effort to achieve an efficient virus-based therapeutics, we previously demonstrated a cancer vaccine regimen combined with intratumor injection of F/M-gene-deleted nontransmissible recombinant Sendai virus (rSeV) expressing interleukin-2 gene in a rat orthotopic model.[10] This was the first experimental protocol to successfully eliminate an established rat 9L gliosarcoma in the brain, and suggested that rSeV would be safe and useful for the clinical practice of glioblastoma therapy. However, because of the highly malignant nature of the 9L tumor, the tumor elimination ratio was modest (~30%) even by this regimen, and there is thus need of a more powerful tool before moving to clinical study.

In order to develop a new therapeutic modality, we returned to the current understanding of the molecular mechanisms involved in the invasive nature of GM, and have recently focused on the protease system. It has been reported that GM frequently expresses urokinase-type plasminogen activator (uPA) and that its

Correspondence: Yoshikazu Yonemitsu, R&D Laboratory for Innovative Biotherapeutics, Graduate School of Pharmaceutical Sciences, Kyushu University, Room 505 Collaborative Research Station II, 3-1-1 Maidashi, Higashi-ku, Fukuoka 812-8582, Japan. E-mail: yonemitu@med.kyushu-u.ac.jp

invasiveness is closely related to uPA activity.[11] uPA can be activated by a high-affinity receptor, uPAR, on the cell surface, after which uPA activates matrix metalloproteases and plasmin, resulting in the degradation of extracellular matrix. Also, activation of these uPA-related proteins induces several intracellular signaling pathways *via* growth factor receptors, thereby facilitating cell adhesion, migration, and proliferation. A number of reports have demonstrated the close relationship between increased levels of local uPA and poor prognosis in cancer patients, including patients bearing GM.[12] Because uPA activity is specifically upregulated in cancerous tissue but not in normal tissue, and uPA activity is observed on the cancer cell surface, it seems reasonable that a therapeutic modality targeting uPA could selectively kill cancer cells without significant damage to the surrounding normal tissue.

To realize this concept, we recently developed novel oncolytic viruses based on a type of rSeV that selectively shows matrix metalloprotease- or uPA-specific cell-killing activity *via* cell–cell fusion,[13,14] namely, "oncolytic rSeV." These new viruses were developed by several major genetic modifications: (i) deletion of the gene encoding matrix (M) protein, which resulted in the loss of budding of secondary viral particles and accumulation of hemagglutinin/neuraminidase and F (fusion) proteins on the cell surface; (ii) replacement of trypsin-susceptible amino acid sequences of the F-gene with targeted protease-specific ones; and (iii) truncation of the cytoplasmic domain of the F-gene. As a result, our recent study demonstrated that uPA-targeted oncolytic rSeV [rSeV/dMFct14(uPA2): named "BioKnife"] showed optimal performance and was applicable to various types of human malignancies.[14]

Therefore, we here examined the therapeutic potential of BioKnife for treating human glioma and a rat orthotopic model of highly malignant 9L gliosarcoma. Our results indicate that BioKnife may be useful for GM treatment. In addition, we revealed that BioKnife armed with the interferon-β (IFN-β) gene exhibited pronounced killing of GM *in vitro* and *in vivo*.

RESULTS

uPA activity–specific cell fusion and killing using BioKnife in human GM cells

In the initial stage of this study, we tested our hypothesis, namely, that uPA activity–dependent cell fusion/killing could be accomplished using infection of the BioKnife vector into five independent lines of human GM cells (U87, U138, U251, U373, and A172) and into a rat 9L gliosarcoma. As shown in **Figure 1a**, a catalytic uPA activity assay revealed that 3 (U138, U251, and U373) of the six cell lines expressed a significant amount of active uPA in culture media. To assess the cytotoxic activity of BioKnife [rSeV/dMFct14(uPA2)] on these cells, a Water-Soluble Tetrazolium (WST) assay was performed. As expected, BioKnife expressing green fluorescent protein (BioKnife-GFP) efficiently killed GM cells that expressed high levels of uPA (U373 and U251; **Figure 1b**, left panels and two graphs). Because modest cytotoxicity due to the M-gene-deleted control recombinant virus (rSeV/dM-GFP, see **Supplementary Figure S1**) was found in U138, A172, and 9L cells, no significant increase in the cytotoxic effect of BioKnife-GFP was detected in these cells. Addition of a sufficient amount of PAI-1, a specific inhibitor for uPA, into the culture medium of U251 cells
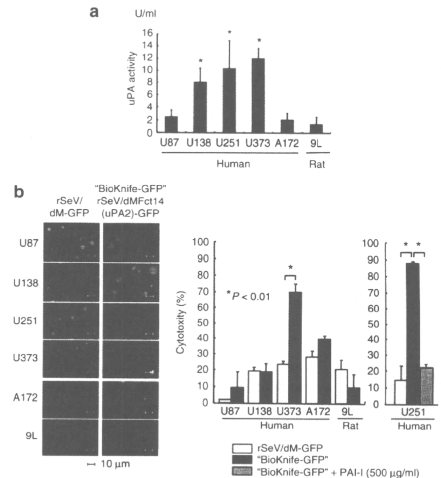

Figure 1 Expression of urokinase-type plasminogen activator (uPA) by human and rat brain tumor cells and their susceptibility to uPA-targeted rSeV/dMFct14(uPA2), namely, BioKnife (*P < 0.01). (a) Expression of uPA by human glioblastoma multiforme cells (U87, U138, U251, U373, and A172) and rat gliosarcoma (9L) in culture medium. Four days after changing to fresh medium, the culture supernatant was subjected to a colorimetric catalytic assay (n = 6 wells/group). (b) Susceptibility of brain tumor cells to BioKnife-GFP or control vector (rSeV/dM-GFP) at an multiplicity of infection of 1.25. Four days after virus inoculation, cells were observed under a fluorescent microscope (panels) and the culture supernatant was subjected to cytotoxicity assay (graphs). In the case of U251, a group with PAI-1, a specific inhibitor of uPA, was included. Note that syncytium formation was observed in wells with U138, U251, U373, or A172 cells (panels), but not in wells with U87 or 9L cells. Significant cytotoxicity was observed against U251 and U373 cells, but not against A172 cells (left graph). Addition of PAI-1 almost completely prevented the BioKnife-dependent cytotoxicity (right graph; n = 6 wells/group).

completely prevented the BioKnife-dependent cytotoxicity (right graph), confirming the uPA-specific killing of U251 cells.

Second, we assessed the time course of the cytotoxicity of BioKnife-GFP and the infection efficiencies based on the rSeV-dM-GFP-positive cell ratio determined by fluorescence-activated cell-sorting analyses on these five human GM cell lines and the rat gliosarcoma cell line 9L. As shown in **Supplementary Figure S2**, even when a small amount of viruses was used (multiplicity of infection = 1.25), the five human cell lines were susceptible to rSeV-dM infection, usually showing an rSeV-dM-GFP-positive cell ratio of over 70%; however, significant and strong cell death was seen only in the cell lines U251 and U373 (see **Figure 1b** for representative results). 9L cells, in contrast, were highly resistant both to rSeV/dM infection and BioKnife-mediated cell death. Together with the data shown in **Figure 1**, these results suggest that uPA activity may predict the cytotoxic activity of BioKnife-GFP, and that the infection efficiency is not always important for BioKnife-mediated cell death.
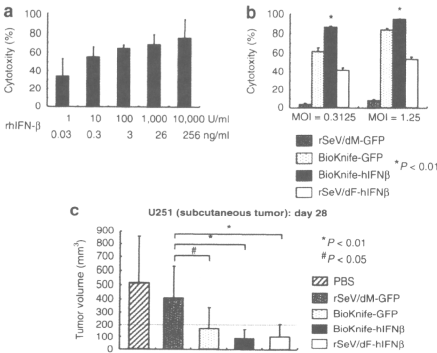
− 290 −

Figure 2 Sole or combined effect of hIFN-β and BioKnife on U251 cells *in vitro* and *in vivo* (*$P < 0.01$ and #$P < 0.05$). (a) Dose-dependent cytotoxic effect of rhIFN-β protein on U251 cells. Four days after addition of various amounts of rhIFN-β, the culture supernatant was subjected to cytotoxicity assay ($n = 4$ wells/group). **(b)** Cytotoxicity due to BioKnife-GFP (rSeV/dM-GFP as a control) and BioKnife-hIFNβ (rSeV/dF-GFP as a control). Four days after exposure of cells to viruses at an MOI of 0.3125 or 1.25, the culture supernatant was subjected to a cytotoxicity assay ($n = 6$ wells/group). **(c)** Antitumor effect of BioKnife-GFP and BioKnife-hIFNβ on U251 tumor cells subcutaneously implanted into the right flank of nude mice. When the subcutaneous tumors grew over 200 mm³ (defined as day 0, usually 14 days after tumor inoculation), 100 µl PBS with or without each vector (1×10^7 cell infection unit/dose) was injected three times (day 0, 3, and 6) intratumorally using a 26-gauge needle. The data indicate the tumor volumes on day 28 after tumor inoculation. MOI, multiplicity of infection; PBS, phosphate-buffered saline; rhIFN-β; recombinant human interferon-β protein.

Next, we focused on U251 cells, which was the only of the human GM cell lines tested that could develop subcutaneous xenograft tumors on immunodeficient mice (data not shown). Also, the effect of BioKnife expressing the human IFN-β gene (hIFN-β) was examined, because hIFN-β has been proven effective for the treatment of experimental and clinical glioma.[15,16] As shown in **Figure 2a**, recombinant hIFN-β protein (rhIFN-β) demonstrated a dose-dependent cytotoxic effect on U251, with over 75% cytotoxicity at 10,000 U/ml (equivalent to 256 ng/ml). A direct comparison study revealed that BioKnife-hIFNβ had a significantly greater cell-killing effect on U251 than any of the other viruses tested (all $P < 0.01$; **Figure 2b**). When U251 cells were implanted on the subcutis of the right flank of *nu/nu* mice, however, the superiority of the antitumor effect of BioKnife-hIFNβ was not apparent, because all the therapies tested were sufficiently effective in this model (**Figure 2c**).

uPA activity on the cellular surface is critical for optimal BioKnife activity

To clarify whether BioKnife shows significant synergism with IFN-β *in vitro* and *in vivo*, we generated 9L cells that were less susceptible to both BioKnife (**Figure 1b**) and recombinant murine IFN-β protein (rmIFN-β; **Figure 4a**) and that stably expressed murine uPA and/or murine uPAR. As shown in **Figure 3a**, western blot analyses
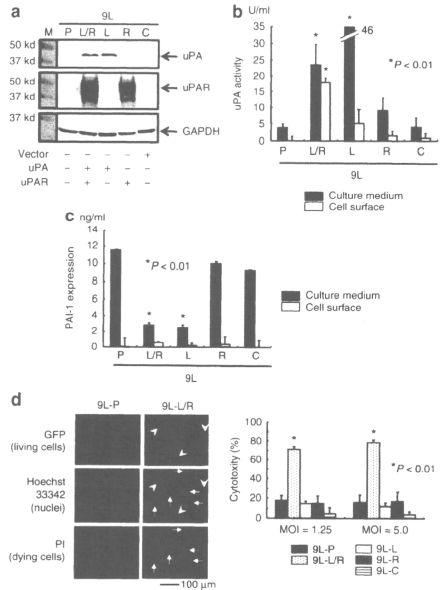
Figure 3 Accumulation of uPA on the cell surface is critical for the biological action of BioKnife (*$P < 0.01$). (a) Representative western blot analyses confirming the protein synthesis stably transfected with murine uPA and/or uPAR cDNA (9L-P: parent 9L; 9L-C: 9L with control plasmid; 9L-L: 9L with uPA ligand cDNA; 9L-R: 9L with uPA receptor cDNA; and 9L-L/R: 9L with both). Three independent experiments were performed and showed similar results. **(b)** Expression of uPA activity in the culture medium and on the cell surface from each transfectant (5×10^5 cells). Forty-eight hours after cell seeding, the supernatant was subjected to the colorimetric uPA activity assay. Both 9L-L/R and 9L-L expressed a high level of uPA in the culture media; however, significant accumulation of uPA activity on the cell surface was seen only in 9L-L/R cells. **(c)** Expression of PAI-1 in the culture medium and on the cell surface from each transfectant. The supernatant obtained in **b** was subjected to enzyme-linked immunosorbent assay for PAI-1. **(d)** Biological activity of BioKnife-GFP forming syncytium (panels, MOI = 1.25) and leading cells to death (graph, MOI = 1.25 and 5.0) on 9L-P or 9L-L/R cells (4 days after virus inoculation). Panels demonstrate the typical fluorescent microscopic findings detecting living cells (expressing foreign GFP genes) and dying cells (positive for PI). Nuclear staining was done using Hoechst 33342. No syncytium formation was found in parent 9L cells (9L-P, three left-hand panels). Note that GFP-expressing multinuclear cells (arrowheads) were negative for PI, and inversely, PI-positive dying cells (arrows) were negative for GFP (three right-hand panels). Two independent experiments were performed and showed similar results. Bar = 100 µm. Graphs represent cytotoxic assay for each transfectant. Only 9L-L/R cells demonstrated a significant increase of susceptibility to BioKnife-GFP ($n = 6$/group). cDNA, complementary DNA; GFP, green fluorescent protein; MOI, multiplicity of infection; PI, propidium iodide; uPA, urokinase-type plasminogen activator.

confirmed that the levels of uPA and uPAR were undetectable in the parent 9L (9L-P), and that the transfected gene-specific protein synthesis had occurred [9L-C: 9L with control plasmid; 9L-L: 9L
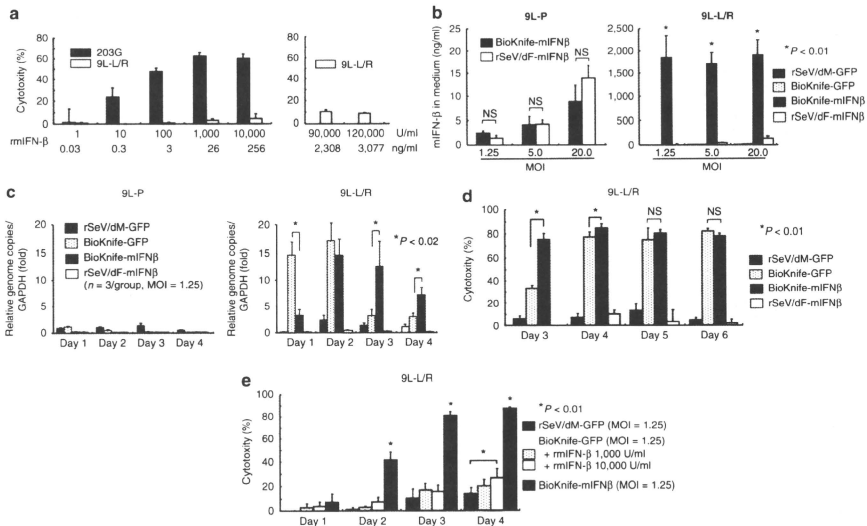
Figure 4 Drastic synergy induced by BioKnife and mIFN-β gene transfer for killing 9L-L/R cells (*P < 0.01). (a) Direct cytotoxic effect of recombinant murine IFN-β (rmIFN-β) on mouse glioma 203G and 9L-L/R cells. Four days after treatment with various amounts of rmIFN-β, a cytotoxicity assay was performed. Note that 203G cells were susceptible to the rmIFN-β protein and dose-dependent cytotoxicity was observed, whereas 9L-L/R cells were highly resistant to rmIFN-β protein even at a concentration of over 90,000 U/ml (equivalent to 2,308 ng/ml). Each group contains n = 4. (b) Cell fusion via BioKnife enhances its mIFN-β transgene expression on 9L-L/R (susceptible to cell fusion, right graph), but not on 9L-P (resistant to cell fusion, left graph). Four days after exposure to each virus at each MOI, the mIFN-β protein level was measured by specific enzyme-linked immunosorbent assay. No significant difference in expression levels was found between rSeV/dF-mIFNβ (nonfusogenic) and BioKnife-mIFNβ (fusogenic) using 9L-P cells (left graph). Note that over 2-logs higher mIFN-β protein levels were found with BioKnife-mIFNβ than with rSeV/dF-mIFNβ at any MOI in 9L-L/R cells (right graph). Significant, but very low levels of mIFN-β protein were detected when using rSeV/dM-GFP and BioKnife-GFP. Each group contains n = 4. (c) Cell fusion via BioKnife potentiates viral genome copies on 9L-L/R (susceptible to cell fusion, right graph), but not on 9L-P (resistant to cell fusion, left graph). After exposure to each virus at an MOI of 1.25 on each time point, viral genome copies were quantified by real-time reverse transcriptase-PCR targeting of the N gene, their common sequence. Each data point was standardized by simultaneous amplification of GAPDH (the genome copies/GAPDH on day 1 in 9L-P cells treated with rSeV/dM-GFP = 1). Strong and early amplification of genome copies of BioKnife-GFP was found in 9L-L/R cells, and declined 3 days after infection. In contrast, delayed and sustained increase of genome copies was found when using BioKnife-mIFNβ. Each group contains n = 3. (d) Arming with the mIFN-β gene accelerates the cytotoxicity of BioKnife to mIFN-β-insensitive 9L-L/R cells. At various time points after exposure to each virus at an MOI of 1.25, a cytotoxicity assay was performed. Note that BioKnife-GFP showed peak cytotoxicity from day 4, whereas BioKnife-mIFNβ had already reached its peak cytotoxicity on day 3. Each group contains n = 6. (e) Acceleration of cell fusion and cytotoxicity due to BioKnife is efficiently induced by mIFN-β gene transfer, but not by rmIFN-β protein. At various time points after exposure to each virus at an MOI of 1.25, a cytotoxicity assay was performed. Note that a modest but significant acceleration of cytotoxicity via BioKnife-GFP was found only in the presence of a high concentration of rmIFN-β (10,000 U/ml) on day 4. GAPDH, glyceraldehyde 3-phosphate dehydrogenase; MOI, multiplicity of infection; NS, nonsignificant; rmIFN-β, recombinant murine interferon-β.

with uPA ligand complementary DNA (cDNA); 9L-R: 9L with uPA receptor cDNA; and 9L-L/R: 9L with both uPA ligand cDNA and uPA receptor cDNA]. Interestingly, only 9L-L/R cells expressed high uPA activity in both the culture medium and on the cell surface, whereas 9L-L cells synthesized uPA only in the culture medium, suggesting that a high level of uPAR expression is required to accumulate active uPA on the cell surface (**Figure 3b**). In contrast, expression of the uPA-specific endogenous inhibitor PAI-1 was almost undetectable on the cell surface of all cells tested, and was significantly downregulated in the culture media of 9L-L/R and 9L-L cells (P < 0.01), suggesting a negative feedback mechanism of uPA or catalytic degradation of PAI-1 by uPA (**Figure 3c**).

Using these cells, we next tested the biological action of BioKnife. As shown in **Figure 3d**, BioKnife-GFP showed optimized cytotoxicity on 9L-L/R cells (**Figure 3d**, graph; P < 0.01). Interestingly, Hoechst 33342 staining (middle two panels) revealed that 9L-L/R cells forming a syncytium contained both living cells strongly expressing the GFP transgene (green, upper two panels, arrowheads) and dying cells stained by propidium iodide (red, lower two panels, arrowheads).

Taken together, these findings indicate that BioKnife shows its optimized biological action—namely, the killing of tumor cells via induction of syncytium formation—when there is a sufficient amount of uPA activity on the cell surface.

Pronounced synergy of BioKnife and the IFN-β transgene for killing of 9L-L/R cells *in vitro*

Next, we examined the synergy between BioKnife and IFN-β for GM therapy using 9L-L/R cells. We here used the mIFN-β gene and recombinant protein (rmIFN-β), because the species-specificity of IFN-β between rodents and humans is widely known. Because our preliminary study showed that the 9L-L/R cell-killing activity of BioKnife expressing the mIFN-β gene (BioKnife-mIFNβ) was superior to that of BioKnife-GFP at 3 days after virus inoculation (data not shown; representative data are shown in **Figure 4d**), we first examined the susceptibility of 9L-L/R cells to BioKnife-mIFNβ.

Recombinant mIFN-β protein (rmIFN-β) showed significant cytotoxicity to 203G murine glioma cells in a dose-dependent manner; however, 9L-L/R cells were highly resistant to rmIFN-β, even when a huge amount of rmIFN-β (~10% of cytotoxicity at 120,000 U/ml, equivalent to 3,077 ng/ml) was used (**Figure 4a**). In addition, inoculation of the conventional nontransmissible vector rSeV/dF-mIFNβ or BioKnife-mIFNβ to parent 9L cells that were resistant to BioKnife-mediated cell fusion produced a similar amount of mIFN-β protein in a dose-dependent manner (**Figure 4b**, left graph). In contrast, we were surprised to observe that the infection of BioKnife-sensitive 9L-L/R cells with BioKnife-mIFNβ dramatically enhanced mIFN-β expression (over 2-logs higher than the expression levels obtained using the others; **Figure 4b**, right graph), indicating that cell fusion markedly accelerated the expression of the transgene.

To seek the possible mechanism underlying the enhanced expression of the mIFN-β transgene, we next assessed the time course of the genome copy numbers of viruses by quantitative real-time reverse transcriptase-PCR (RT-PCR) targeting the N gene. In the case of the SeV, it is well known that genome replication reflects its transcription well. As shown in **Figure 4c**, cell fusion *via* BioKnife potentiates the number of viral genome copies on 9L-L/R (susceptive to cell fusion, right graph), but not on 9L-P (resistant to cell fusion, left graph). Interestingly, strong and early amplification of genome copies of BioKnife-GFP was found in 9L-L/R cells, and declined 3 days after infection. In contrast, a delayed and sustained increase of genome copies was found when using BioKnife-mIFNβ. It was suggested, therefore, that this sustained increase of genome copies and its transcription might have resulted in the enhanced IFN-β transgene expression shown in **Figure 4b**.

Next, we questioned the reverse effect—in other words, whether BioKnife-mIFNβ might accelerate cell fusion and killing even in mIFN-β-insensitive 9L-L/R cells. To examine this hypothesis, we checked the cytotoxicity over a time course. Interestingly, the cytotoxicity induced by BioKnife-GFP peaked on days 4–5, whereas cells treated with BioKnife-mIFNβ already demonstrated a nearly peak cell death on day 3 (**Figure 4d**). Then, we asked whether the transgene expression of mIFN-β might accelerate the cell fusion/killing and whether rmIFN-β might have an effect similar to that seen using the transgene. As shown in **Figure 4e**, a pronounced acceleration of cytotoxicity on 9L-L/R was observed when using BioKnife-mIFNβ. In contrast, a modest enhancement of cell-killing by BioKnife-GFP was seen under a higher concentration of rmIFN-β on day 4, indicating the drastic improvement in the biological activity of BioKnife conferred by transgene expression of the mIFN-β gene.
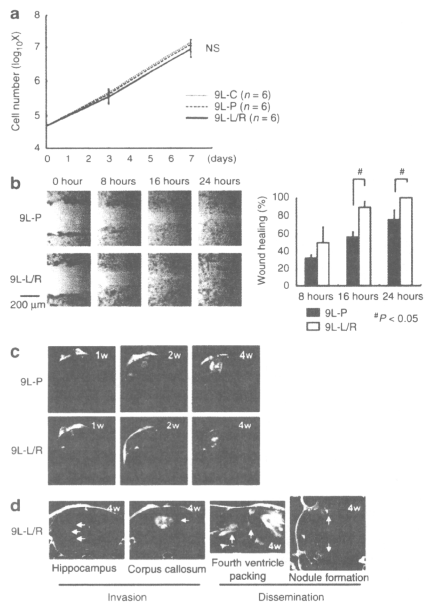

Figure 5 **Overexpression of urokinase-type plasminogen activator (uPA)/uPA facilitates the invasive potential of 9L gliosarcoma cells.** (**a**) Growth curve of 9L-L/R cell *in vitro*. No significant difference was found between 9L-P and 9L-C. (**b**) Wound-healing assay of 9L-P and 9L-L/R cells for assessing cell migration activity *in vitro*. A single linear wound was made with a 200 μl pipette, and each wound area was calculated 8, 16, and 24 hours later. Left panels are the representative phase-contrast images. Facilitated wound repair was found in 9L-L/R cells, indicating that the overexpression of uPA/uPA accelerates cell migration activity. (**c,d**) Time course of the growth and invasiveness of 9L-P (n = 12 animals) or 9L-L/R (n = 15 animals) cells in rat brains assessed by sequential assessment with magnetic resonance imaging (MRI). (**c**) All rats inoculated with 9L-P cells and 10 rats inoculated with 9L-L/R cells showed local growth around the injection site with neither detectable invasion nor dissemination. (**d**) A typical MR image showing invasion and dissemination. Five rats receiving 9L-L/R cells showed invasive cell transfer that included: (i) direct progression along neural fibers of the hippocampus and/or corpus callosum; (ii) cerebrospinal fluid dissemination surrounding the cerebral ventricle and/or forming nodules on the brain surface. NS, nonsignificant.

Pronounced synergy of BioKnife and the IFN-β transgene for killing of 9L-L/R cells *in vivo*

Before the *in vivo* study assessing the therapeutic potentials of BioKnife, we investigated the effect of forced uPA/uPAR gene expression on the growth and behavior of 9L cells *in vitro* and *in vivo*. As shown in **Figure 5a**, the growth activity of 9L-L/R *in vitro* was identical to those of 9L-P and 9L-C. In contrast, the *in vitro* wound-healing assay revealed the significantly enhanced migratory activity of 9L-L/R cells (**Figure 5b**). Magnetic resonance imaging (MRI) also demonstrated that the local growth of 9L-L/R
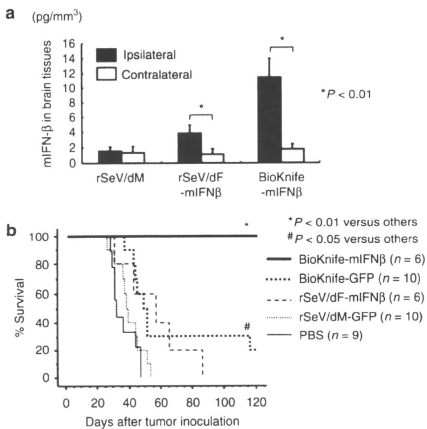
Figure 6 Impact of BioKnife expressing the mIFN-β gene for the treatment of an orthotopic rat brain tumor model with 9L-L/R (*P < 0.01 and *P < 0.05). (a) mIFN-β expression in ipsilateral (tumor bearing) and contralateral (no tumor) brain tissues 2 days after a single intratumor injection of BioKnife-mIFNβ or control vectors [rSeV/dM and rSeV/dF-mIFNβ; 1 × 10⁷ cell infection unit (CIU)/dose]. Each group contains n = 8 animals. **(b)** Therapeutic effect of BioKnife-mIFNβ on an orthotopic rat brain tumor model. On days 1, 4, and 7 after tumor injection, each virus (2 × 10⁷ CIU) in 20 µl PBS was injected, and the cell survival was observed. The data are the sum of two independent experiments. mIFN-β, murine interferon-β; PBS, phosphate-buffered saline.

tumors in the rat brain *in vivo* was roughly identical to that seen with 9L-P tumors (**Figure 5c**; 9L-P: n = 12 animals; 9L-L/R: n = 15 animals); however, five animals that received 9L-L/R cells showed the invasive growth of tumors to the hippocampus and/or corpus callosum, as well as the tumor dissemination to the fourth ventricle packing and/or nodule formation at the distant central nervous system (**Figure 5d**), indicating that forced expression of uPA/uPAR resulted in the increased malignant potential of 9L tumors.

Pronounced synergy of BioKnife and the IFN-β transgene for killing of 9L-L/R cells *in vivo*

Finally, the therapeutic potential of BioKnife-mIFNβ on an orthotopic rat model of GM was investigated using 9L-L/R cells. We first assessed the expression level of transgene mIFN-β *in vivo* in 9L-L/R tumor-bearing rat brain tissue. Two days after injection of vector at 1 × 10⁷ cell infection unit (CIU)/dose, the brain tissue was subjected to specific enzyme-linked immunosorbent assay (ELISA). As shown in **Figure 6a**, strong enhancement of transgene expression was found when using BioKnife-mIFNβ as compared to that seen using rSeV/dF-mIFNβ at the ipsilateral site, and the findings were similar to those seen in the *in vitro* experiment (**Figure 4b**).

The therapeutic benefit on the survival of tumor-bearing rats is shown in **Figure 6b**; all control rats that were treated with phosphate-buffered saline (PBS) or nonfusogenic rSeV/dM-GFP

were dead within 46 or 52 days after tumor inoculation, respectively. Gene transfer of mIFN-β *via* rSeV/dF significantly improved the survival of rats with IFN-β-insensitive 9L-L/R (P < 0.05), suggesting that this therapeutic effect might have been due to the well-known immune-mediated antitumor effect of IFN-β, but not due to its direct cytotoxicity on tumor cells. Similarly, the survival of tumor-bearing rats that received BioKnife-GFP was also significantly prolonged compared to those in the PBS or rSeV/dM-GFP group (P < 0.05, respectively). Compared to these efficacies, BioKnife-mIFNβ showed a dramatic enhancement of the therapeutic potential of BioKnife: namely, no dead animals were observed during the trial. These surviving rats exhibited no residual tumor cells in their brain tissue either macroscopically or microscopically (data not shown).

These results provided clear evidence of a pronounced synergistic effect between the fusogenic activity of BioKnife and the IFN-β transgene *in vitro* and *in vivo*.

DISCUSSION

Here, we investigated the potential and mechanism of our recently developed uPA-targeted oncolytic virus, BioKnife, to treat a rat model of GM. Key observations obtained in this study were as follows: (i) among 9L cells that were stably transformed with the uPA and/or uPAR gene, accumulation of uPA activity on the cellular surface was crucial for the optimal biological functioning of BioKnife; (ii) there was a dramatic synergy between cell fusion/cytotoxicity and IFN-β transgene expression *via* BioKnife—namely, we observed an acceleration of cell fusion and a dramatic increase of transgene expression; and (iii) the synergistic effects of BioKnife-IFNβ were effective for treating a rat orthotopic brain tumor model with 9L-L/R, even if the tumor itself was resistant to IFN-β therapy alone. These findings indicate the potential utility of BioKnife expressing the IFN-β gene and provide important information related to the biological parameters predicting the efficacy of BioKnife in future clinical trials.

During the course of this study, we had some unexpected findings; however, some of these anomalies were resolved in subsequent experiments. First, the expression level of uPA did not always predict the cytotoxic activity of BioKnife (e.g., U138, **Figure 1**), and this question was resolved by an experiment using 9L, which showed that the cell surface accumulation of uPA, but not its release, was critical for the biological activity of BioKnife (**Figure 3**). To the best of our knowledge, this is the first demonstration that the expression of uPAR is critical for facilitating the accumulation of active uPA on the cell surface. Second, although BioKnife-GFP appeared to be capable of facilitating syncytium formation of U138 and U172 (**Figure 1b**, panels), the observed cytotoxicity did not always support the notion that such syncytium formation occurred (**Figure 1b**, graphs). This contradictory data could be explained by the data in **Figure 3d**: namely, syncytium formation did not always correlate with dying cells, at least at this time point.

Next, we should discuss why PAI-1 expression in the culture media from 9L-L/R and 9L-L was downregulated, as it was previously shown that uPA enhances the expression of PAI-1.[17] A possible explanation for this paradox is that the uPA/PAI-1 complex may mask epitopes recognized by the ELISA system,

because RT-PCR analysis could not detect a significant reduction of PAI-1 mRNA in these cells (data not shown).

A most important question remains—namely, by what mechanism is the dramatic synergy between BioKnife and the IFN-β transgene realized? It has been widely accepted based on previous studies[18,19] that type-I IFNs inhibit cell–cell fusion and viral replication of paramyxoviruses, including SeV. However, our data obtained by recombinant viruses suggest that this rule may not apply in all situations; for example, the recombinant virus yield during the amplification process of BioKnife encoding IFN-β using LLC-MK2 cells is significantly increased more than severalfold compared with that of BioKnife expressing other transgenes (unpublished results). Interestingly, the cell–cell fusion of epithelial and dendritic cells induced by measles virus, a member of *Paramyxoviridae*, was shown to be enhanced by type-I IFNs,[20] suggesting that acceleration of the cell–cell fusion induced by IFN-β might be cell- and/or species-specific. In this study, we also found that BioKnife-mediated cell–cell fusion strongly enhanced IFN-β transgene expression, which reached over 2-logs higher than that seen when using nonfusogenic virus. Because the transgene of BioKnife was expressed by its own viral expression machinery, these findings theoretically indicate that cell–cell fusion facilitates viral protein synthesis; however, to the best of our knowledge, there has been no published data that could explain these findings. Therefore, further studies will be needed to investigate the molecular mechanisms of such synergies.

Finally, because *in vivo* experiments using the orthotopic GM model in this study demonstrated a dramatic therapeutic effect, the clinical relevance of our BioKnife-IFNβ should be discussed. First, almost all surgical specimens of GM were shown to express a high level not only of biologically active uPA but also uPAR,[21,22] suggesting that a majority of GM patients would be good candidates for this therapeutics. The current model may be clinically relevant to residual and disseminated tumor cells rather than solid tumors, because virus injection was started 1 day after tumor inoculation; therefore, the adjuvant use of BioKnife-IFNβ after mass reduction *via*, for example, surgery and/or stereotactic radiotherapy would be reasonable. Although it may be possible that such a protease-targeting strategy would show limited efficacy, because urokinase is variably expressed at different sites in the parenchyma of growing tumors, these theoretical considerations based on this study warrant further investigations and encouraged us to move this system to the clinic.

In conclusion, we here demonstrated the efficient control of a rat orthotopic model of GM *via* the marked synergistic actions of IFN-β gene transfer and BioKnife, an oncolytic rSeV targeting uPA. These findings support the therapeutic potential of BioKnife-IFNβ for intractable GM in a clinical setting.

MATERIALS AND METHODS

Cells, reagents, ELISA, plasmid vectors. The human brain tumor cell lines (U87, U138, U251, U373, and A172) and the rat cell line 9L were purchased from American Type Culture Collection (Rockville, MD) or the European Collection of Cell Cultures (England, UK). These cell lines were maintained in complete medium (RPMI 1640 for 203G and Dulbecco's modified Eagle's medium for the others) supplemented with 10% fetal bovine serum, penicillin, streptomycin, and 1% sodium pyruvate (Flow Laboratories, Mclean, VA) under a humidified atmosphere containing

5% CO_2 at 37 °C. ELISA was performed using commercially available kits for rat PAI-1 (Hyphen Biomed, Andresy, France) and for mIFN-β (PBL Biomedical Laboratories, Piscataway, NJ). Full-length murine upA and uPAR cDNAs were cloned from total RNA of Lewis lung cancer cells (American Type Culture Collection: CRL-1642) by RT-PCR, and human uPA and uPAR cDNAs were cloned from total RNA of human prostate tumor cells: PC3 (American Type Culture Collection: CRL-1435) by RT-PCR. The sequences of PCR primers with BamHI and NheI sites were the following: murine upA, forward 5'-TCTAGCTAGCCGCCATGAAAG TCTGGCTGG CGAGC-3'/reverse 5'-CCGCGGATCCTCAGAAGGCCA GACCTTTCTC-3'; murine uPAR, forward 5'-TCTAGCTAGCCGCCAT GGGACTCCCAAGGCGGCTG-3'/reverse 5'-CCGCGGATCCTCAGGT CCAGAGGAGGACGCC-3'). Amplified cDNA fragments were digested with BamHI and NheI and inserted into a pcDNA3.1 vector (Invitrogen, Carlsbad, CA). The full sequences of cDNAs were determined by direct sequencing.

Construction and recovery of BioKnife vectors. rSeVs and rSeV armed with IFN-β were constructed as described previously,[13,14,23] and all schematic structures of viruses used in this study are demonstrated in the **Supplementary Figure S1**. In brief, the parent plasmid pSeV18+/dM-GFP, in which the GFP had been substituted for the deleted M gene,[24] was digested with SalI and NheI, and the F-gene fragment (9,634 bp) was subcloned into LITMUS 38 (New England Biolabs, Beverly, MA). Site-directed mutagenesis was performed using a Quick-Change Mutagenesis Kit (Stratagene, La Jolla, CA), and the mutated F-gene was returned to the pSeV18+/dF-GFP backbone. mIFN-β and hIFN-β cDNAs were previously cloned[25] and were inserted into the pSeV18+/Fct14(uPA2)dM-GFP plasmid. Recovery and amplification of the SeV vector were performed essentially as described before. Briefly, LLC-MK2 cells were transfected with a plasmid mixture containing each plasmid—pSeV18+/Fct14 (uPA2) dM-GFP, pGEM-NP, pGEM-P, and pGEM-L—in 110 µl of Superfect reagent (Qiagen, Tokyo, Japan). The transfected cells were maintained for 3 hours, washed three times, and incubated for 60 hours in minimum essential medium containing araC. The cells were collected and lysed by three cycles of freezing and thawing. The lysate solution was incubated on the F/M-expressing LLC-MK2 cells in a 24-well plate. Twenty-four hours later, the cells were washed and incubated in minimum essential medium containing araC and 7.5 µg/ml trypsin plus 10 ng/ml urokinase (Cosmobio, Tokyo, Japan). The virus yield was expressed in CIU, as previously described.[13,14] Expression of mIFN-β or hIFN-β was determined by specific ELISA.

Virus titration. The virus titers were expressed as CIU, which were estimated by infecting confluent LLC-MK2 cells in a 6-well plate with diluted solution as previously described.[13,14] In brief, LLC-MK2 cells were inoculated in duplicate with a series of dilutions of virus, then incubated for 1 hour and washed twice with PBS. Two days after infection, cells were fixed in methanol, incubated with anti-SeV primary antibodies, and then incubated with fluorescein isothiocyanate–labeled goat anti-rabbit IgG(H+L) (Invitrogen). Immunofluorescent-positive cell were counted and CIU/ml were calculated.

uPA activity assay and ELISA for PAI-1 and mIFN-β. Cells (1.5×10^4) in 60 µl medium were seeded in a 96-well dish, and the supernatants were collected after 48 hours. The uPA activity or PAI-1 expression in the culture medium and on the cell surface of denucleated cells that were washed three times with a sufficient amount of PBS was measured using a colorimetric uPA Activity Assay Kit (Chemicon International, Temecula, CA) or ELISA kit for rat PAI-1, according to the manufacturer's instruction.

Cytotoxicity assay. Cells (5×10^3) were seeded in a 96-well dish with 100 µl medium containing various concentrations of recombinant hIFN-β (PBL Biomedical Laboratories), mIFN-β (Chemicon International)

proteins, or various amounts of viruses. At each time point, cytotoxicity was measured using a Premix WST-1 Cell Proliferation Assay System (Takara Bio, Otsu, Japan). Defining the cell viability of a negative control well as 100%, the cytotoxicity of each well was calculated by subtracting the corresponding viability from 100%.

uPA- and/or uPAR-expressing stable transfectants of 9L. 9L cells (3×10^5) were seeded in 6-well dishes with 2 ml medium/well, and the following day, the plasmid vectors were transfected using TransIT-LT1 Reagent (Mirus Bio, Madison, WI) according to the manufacturer's instructions. Gene-transferred 9L cells (9L-P: parent 9L; 9L-C: 9L with control plasmid; 9L-L: 9L with uPA ligand cDNA; 9L-R: 9L with uPA receptor cDNA; and 9L-L/R: 9L with both uPA ligand cDNA and uPA receptor cDNA) were maintained under 200 μg/ml of antibiotic G-418, and the clones surviving from single cells were selected twice.

Western blotting. Samples were lysed in lysis buffer containing 50 mmol/l Tris–HCl (pH 6.8) and 10% sodium dodecyl sulfate, and the protein concentration for each sample was determined by using a Bio-Rad Protein Assay kit (Bio-Rad Laboratories, Hercules, CA). Anti-mouse uPA (ab20789, rabbit, 1:1,000; Abcam, Cambridge, UK), anti-mouse uPAR (AF534, goat, 1:1,000; R&D Systems, Abingdon, UK), and anti-glyceraldehyde 3-phosphate dehydrogenase (IMG-5143A, rabbit, 1:1,000; IMGENEX, San Diego, CA) were used as primary antibodies. The secondary antibodies, anti-rabbit IgG (65-6120, goat, 1:10,000; Invitrogen) or anti-goat IgG (561-71271, rabbit, 1:10,000; Jackson ImmunoResearch Laboratories, West Grove, PA), were applied for 30 minutes. Specific bands were visualized using an ECL Plus Western Blotting Detection System (GE Healthcare, Little Charfont, UK).

Quantitative real-time RT-PCR assessing rSeV genome copies. Total cellular RNA was extracted from cultured cells with an ISOGEN system (Wako Pure Chemicals, Tokyo, Japan) according to the manufacturer's instructions, then treated with RNase-free DNAase I (Boehringer Mannheim, Mannheim, Germany). A volume of 25 ng of total RNA was subjected to real-time RT-PCR. Real-time monitoring of the amplification and quantification of genome copies of rSeV were done using a model 7000 Sequence Detection System (Applied Biosystems, Tokyo, Japan) by the TaqMan method according to the manufacturer's instructions. The oligonucleotide sequences of PCR primers and TaqMan probes targeting the N gene (forward: 5′-CAATGCCGACATCGACCTAGA-3′; reverse: 5′-CGTGCCCATCTTTCACCACTA-3′; TaqMan Probe: FAM-ACAAAAGCCCATGCGGACCAGGAC-TAMRA), a common sequence for all vector constructs used in this study, were purchased from Applied Biosystems. Three independent experiments were performed and the obtained data were statistically analyzed. The genome copies were standardized by the glyceraldehyde 3-phosphate dehydrogenase level in each sample, and expressed as a relative fold increase compared with the control level.

Wound-healing assay. A single linear wound was made with a 200 μl pipette tip in confluent cultures of 9L-P or 9L-L/R cells and washed gently with PBS to remove cellular debris. The cells were transferred to fresh medium and incubated at 37 °C. After 8, 16, and 24 hours, the cells were photographed and the area of each wound was calculated.

Animals. Female 7- to 8-week-old Balb/c *nu/nu* mice and male Fisher 344 rats were obtained from the Shizuoka Laboratory Animal Center. Animals were kept under specific pathogen-free and humane conditions in the animal care facility of Chiba University's Inohana campus. The animal experiments were reviewed and approved by the Institutional Animal Care and Use Committee and by the Biosafety Committee for Recombinant DNA experiments of Chiba University. These experiments were also done in accordance with the recommendations for the proper care and use of laboratory animals and according to The Law (no. 105) and Notification (no. 6) of the Japanese Government.

Subcutaneous tumor model of human U251 cells in nu/nu mice: A density of 1×10^7 U251 cells in 50 μl PBS plus 50 μl Matrigel (BD Biosciences, Bedford, MA) were subcutaneously injected into the right flank of nude mice. The tumor volume was calculated every 3 or 4 days, until day 28 after tumor inoculation, using the following formula: volume = $a^2b/2$, where *a* is the shortest diameter and *b* is the longest. When the subcutaneous tumors grew over 200 mm³ (defined as day 0, usually 14 days after tumor inoculation), the mice were divided into treatment or control groups, and 100 μl PBS with or without each vector (1×10^7 CIU/dose) was injected 3 times (day 0, 3, and 6) intratumorally using a 26-gauge needle.

Orthotopic GM model of 9L-L/R cells in rats: A density of 5×10^5 9L-L/R cells with 10 μl PBS were injected into rat brains using a microinjector (Harvard Apparatus, South Natick, MA) over 5 minutes, as previously described.[10] Briefly, rats were anesthetized with 50 mg/kg pentobarbital and placed in a stereotactic apparatus. A burr hole was made at an appropriate location (1 mm posterior to the bregma and 3 mm right to the midline). A 25-gauge needle was inserted at a point 3 mm ventral from the dura. On days 1, 4, and 7 after tumor injection, each SeV vector (2×10^7 CIU) with 20 μl PBS was injected in the same way. In addition, to evaluate the invasive activity of 9L-L/R, 1×10^5 of 9L-P or 9L-L/R cells with 10 μl PBS were injected into other rat brain in the same way and examined every 7 days using MRI. The invasive activity was measured at 4 weeks after tumor inoculation. The rats were observed daily until severe paresis, ataxia periophthalmic encrustations, or >20% weight loss developed.

MRI. All rats were anesthetized with 2.0% isoflurane (Abbott Japan, Tokyo, Japan) and injected with 0.4 ml of Gd-DTPA (Meglumine Gadopentetate, 0.002 ml/g, 50 mmol/l, Bayer, Leverkusen, Germany) intravenously 15 minutes before MRI measurement. All MRI experiments were performed on a 7.0-T MRI scanner (Magnet: Kobelco and JASTEC, Kobe, Japan; Console: Bruker Biospin, Ettlingen, Germany) with a volume coil for transmission (Bruker Biospin) and two-channel phased array coil for reception (Rapid Biomedical, Rimpar, Germany). Multislice T_1-weighted MR images covering the entire brain (T1WI; multislice spin echo, TR/TE = 400/9.57 ms, slice thickness = 1.0 mm, slice gap = 0, number of slices = 16, matrix = 256 × 256, field of view = 25.6 × 25.6 mm², average = 4) were acquired. The slice orientation was transaxial for all scans. Two independent neurosurgeons evaluated the MRIs to determine whether either "invasion" or "dissemination" were present. "Invasion" was defined as direct progression along neural fiber tracts and "dissemination" was defined as distant tumor growth separated from the original injection site by cerebrospinal fluid. When either invasion or dissemination was clearly observed in the transaxial plane, images in the horizontal and sagittal planes were also acquired. Image reconstruction and analysis were performed using ParaVision (Bruker Biospin).

Statistical analysis. All data were expressed as the means ± SD. The data were examined statistically using one-way analysis of variance with Scheffe adjustment. When the number of evaluated groups was small, the data were subjected to the Kruskal–Wallis or Mann–Whitney *U* test. The survival curves were determined using the Kaplan–Meier's method. The log-rank test was used for comparison. A probability value of $P < 0.05$ was considered statistically significant. Statistical analyses were determined using StatView software (SAS Institute, Cary, NC).

SUPPLEMENTARY MATERIAL
Figure S1. The structures of BioKnife and its relatives used in this study.
Figure S2. Cytotoxic activities of BioKnife-GFP on various human glioblastomas and rat 9L gliosarcoma.

REFERENCES

1. DeAngelis, LM (2001). Brain tumors. *N Engl J Med* **344**: 114–123.
2. Stupp, R, Mason, WP, van den Bent, MJ, Weller, M, Fisher, B, Taphoorn, MJ *et al.*; European Organisation for Research and Treatment of Cancer Brain Tumor and Radiotherapy Groups; National Cancer Institute of Canada Clinical Trials Group. (2005). Radiotherapy plus concomitant and adjuvant temozolomide for glioblastoma. *N Engl J Med* **352**: 987–996.
3. Brandes, AA, Tosoni, A, Franceschi, E, Sotti, G, Frezza, G, Amistà, P *et al.* (2009). Recurrence pattern after temozolomide concomitant with and adjuvant to radiotherapy in newly diagnosed patients with glioblastoma: correlation With MGMT promoter methylation status. *J Clin Oncol* **27**: 1275–1279.
4. Rainov, NG (2000). A phase III clinical evaluation of herpes simplex virus type 1 thymidine kinase and ganciclovir gene therapy as an adjuvant to surgical resection and radiation in adults with previously untreated glioblastoma multiforme. *Hum Gene Ther* **11**: 2389–2401.
5. Liu, TC, Galanis, E and Kirn, D (2007). Clinical trial results with oncolytic virotherapy: a century of promise, a decade of progress. *Nat Clin Pract Oncol* **4**: 101–117.
6. Yokoyama, T, Iwado, E, Kondo, Y, Aoki, H, Hayashi, Y, Georgescu, MM *et al.* (2008). Autophagy-inducing agents augment the antitumor effect of telerase-selve oncolytic adenovirus OBP-405 on glioblastoma cells. *Gene Ther* **15**: 1233–1239.
7. Wakimoto, H, Kesari, S, Farrell, CJ, Curry, WT Jr, Zaupa, C, Aghi, M *et al.* (2009). Human glioblastoma-derived cancer stem cells: establishment of invasive glioma models and treatment with oncolytic herpes simplex virus vectors. *Cancer Res* **69**: 3472–3481.
8. Liu, C, Sarkaria, JN, Petell, CA, Paraskevakou, G, Zollman, PJ, Schroeder, M *et al.* (2007). Combination of measles virus virotherapy and radiation therapy has synergistic activity in the treatment of glioblastoma multiforme. *Clin Cancer Res* **13**: 7155–7165.
9. Piao, Y, Jiang, H, Alemany, R, Krasnykh, V, Marini, FC, Xu, J *et al.* (2009). Oncolytic adenovirus retargeted to Δ-EGFR induces selective antiglioma activity. *Cancer Gene Ther* **16**: 256–265.
10. Iwadate, Y, Inoue, M, Saegusa, T, Tokusumi, Y, Kinoh, H, Hasegawa, M *et al.* (2005). Recombinant Sendai virus vector induces complete remission of established brain tumors through efficient interleukin-2 gene transfer in vaccinated rats. *Clin Cancer Res* **11**: 3821–3827.
11. Rao, JS (2003). Molecular mechanisms of glioma invasiveness: the role of proteases. *Nat Rev Cancer* **3**: 489–501.
12. Zhang, X, Fei, Z, Bu, X, Zhen, H, Zhang, Z, Gu, J *et al.* (2000). Expression and significance of urokinase type plasminogen activator gene in human brain gliomas. *J Surg Oncol* **74**: 90–94.
13. Kinoh, H, Inoue, M, Washizawa, K, Yamamoto, T, Fujikawa, S, Tokusumi, Y *et al.* (2004). Generation of a recombinant Sendai virus that is selectively activated and lyses human tumor cells expressing matrix metalloproteinases. *Gene Ther* **11**: 1137–1145.
14. Kinoh, H, Inoue, M, Komaru, A, Ueda, Y, Hasegawa, M and Yonemitsu, Y (2009). Generation of optimized and urokinase-targeted oncolytic Sendai virus vectors applicable for various human malignancies. *Gene Ther* **16**: 392–403.
15. Mizuno, M and Yoshida, J (1998). Effect of human interferon beta gene transfer upon human glioma, transplanted into nude mouse brain, involves induced natural killer cells. *Cancer Immunol Immunother* **47**: 227–232.
16. Colman, H, Berkey, BA, Maor, MH, Groves, MD, Schultz, CJ, Vermeulen, S *et al.*; Radiation Therapy Oncology Group. (2006). Phase II Radiation Therapy Oncology Group trial of conventional radiation therapy followed by treatment with recombinant interferon-beta for supratentorial glioblastoma: results of RTOG 9710. *Int J Radiat Oncol Biol Phys* **66**: 818–824.
17. Shetty, S, Bdeir, K, Cines, DB and Idell, S (2003). Induction of plasminogen activator inhibitor-1 by urokinase in lung epithelial cells. *J Biol Chem* **278**: 18124–18131.
18. Tomita, Y and Kuwata, T (1981). Suppressive effects of interferon on cell fusion by Sendai virus. *J Gen Virol* **55**(Pt 2): 289–295.
19. Chatterjee, S, Cheung, HC and Hunter, E (1982). Interferon inhibits Sendai virus-induced cell fusion: an effect on cell membrane fluidity. *Proc Natl Acad Sci USA* **79**: 835–839.
20. Herschke, F, Plumet, S, Duhen, T, Azocar, O, Druelle, J, Laine, D *et al.* (2007). Cell-cell fusion induced by measles virus amplifies the type I interferon response. *J Virol* **81**: 12859–12871.
21. Yamamoto, M, Sawaya, R, Mohanam, S, Rao, VH, Bruner, JM, Nicolson, GL *et al.* (1994). Expression and localization of urokinase-type plasminogen activator receptor in human gliomas. *Cancer Res* **54**: 5016–5020.
22. Landau, BJ, Kwaan, HC, Verrusio, EN and Brem, SS (1994). Elevated levels of urokinase-type plasminogen activator and plasminogen activator inhibitor type-1 in malignant human brain tumors. *Cancer Res* **54**: 1105–1108.
23. Li, HO, Zhu, YF, Asakawa, M, Kuma, H, Hirata, T, Ueda, Y *et al.* (2000). A cytoplasmic RNA vector derived from nontransmissible Sendai virus with efficient gene transfer and expression. *J Virol* **74**: 6564–6569.
24. Inoue, M, Tokusumi, Y, Ban, H, Kanaya, T, Shirakura, M, Tokusumi, T *et al.* (2003). A new Sendai virus vector deficient in the matrix gene does not form virus particles and shows extensive cell-to-cell spreading. *J Virol* **77**: 6419–6429.
25. Shibata, S, Okano, S, Yonemitsu, Y, Onimaru, M, Sata, S, Nagata-Takeshita, H *et al.* (2006). Induction of efficient antitumor immunity using dendritic cells activated by recombinant Sendai virus and its modulation by exogenous IFN-β gene. *J Immunol* **177**: 3564–3576.